



CHALMERS
UNIVERSITY OF TECHNOLOGY



A Chalmers University of Technology Bachelor's thesis

Researching possibilities for autonomous operation of a Sigfox
radio base station north of the Arctic circle

Bachelor thesis in Electrical engineering
Examensarbete för Högskoleingenjör inom Elektroteknik

Emil Eskång & Gustaf Dahl

BACHELOR'S THESIS 2018:06

Researching possibilities for autonomous operation of a Sigfox radio base station north of the Arctic circle

Undersökning av möjligheterna för autonom drift av en Sigfox radiobasstation
norr om polcirkeln

Emil Eskång & Gustaf Dahl



CHALMERS
UNIVERSITY OF TECHNOLOGY

Department of Electrical Engineering
CHALMERS UNIVERSITY OF TECHNOLOGY
Gothenburg, Sweden 2018

**Researching possibilities for autonomous operation of a Sigfox radio base station
north of the Arctic circle**

Emil Eskång & Gustaf Dahl

© Emil Eskång & Gustaf Dahl, 2018.

Supervisor: Mikael Falkvidd, Falkvidd Holding & Arni Alfredsson, Department of Electrical Engineering, Division of Communication and Antenna systems

Examiner: Prof. Tommy Svensson, Department of Electrical Engineering, Division of Communication and Antenna systems

Bachelor's Thesis 2018:06

Department of Electrical engineering

Chalmers University of Technology

SE-412 96 Gothenburg

Telephone +46 31 772 1000

Cover: Photomontage showing the Tarfala valley with a possible placement of an autonomous base station. Picture by Gustaf Dahl, 2016.

Typeset in L^AT_EX

Printed by [Chalmers Reproservice]

Gothenburg, Sweden 2018

Abstract

This project analyses the possibilities of powering a Sigfox *LPWAN* (Low-Power Wide-Area Network) base station using solar power, while operating north of the Arctic circle throughout the year. Basic theory of photovoltaics and lead-acid battery technology are described in order to provide an understanding of which key factors to think of when designing a solar powered solution for the difficult conditions faced in this environment.

LPWAN is a fast growing technology within the field of *IoT* (Internet of Things). LPWAN enables sensors to transmit small data packages over large distances in a power efficient- and low maintenance fashion. The possibility to communicate over large distances allows placement of gauges and sensors in remote places and due to the low power consumption of the endpoint devices a unit can stay functional for several years without the need for regular maintenance and human interference. This creates an opportunity for effective and autonomous data gathering that can help to monitor large unsupervised areas. However, to create this opportunity, the LPWAN network coverage has to be extended.

On the request of IoT Sweden we have analysed the possibilities of providing Sigfox LPWAN network coverage for "*off-the-grid areas*" north of the Arctic circle, which lack electrical grid connectivity.

The goal is to determine what is needed to ensure that a Sigfox SBS-T3-868 base station can stay operational in these areas throughout the year. To be able to create an optimised system, the design and calculations are based on the surroundings of the Tarfala area above the Arctic circle.

The result concluded that there is no beneficial way of designing a solar powered system for the Sigfox SBS-T3-868 base station in any parts of the Nordic countries, much less north of the Arctic circle. This is mainly due to the high power consumption of the base station. The result also presents theory and tools relevant when designing a smaller solar powered system for use north of the Arctic circle. Solar power is the only energy source that has been studied due to the fact that it is a low-maintenance technology with no moving parts and a long lifespan. Furthermore, improvements are discussed, mainly focusing on the consumption of the base station.

Keywords: LPWAN, Sigfox, IoT Sweden, solar powered, battery, autonomous.

Acknowledgements

We would like to thank the people at IoT Sweden and Diginav for giving us the opportunity to research this field and learn more about the LPWAN technology, solar powered systems and the future of data gathering. In particular Carina Dahlberg and Peter Selemark for their insights and willingness to help.

We would also like show our gratitude to our supervisors Mikael Falkvidd and Arni Alfredsson, as well as examiner Tommy Svensson for providing great support and showing a big interest in this project.

Our gratitude also includes the people behind the SMHI and POWER project databases, as well as all the researchers, engineers and people that have written the books, articles and papers used by us for the research in this project.

Emil Eskång & Gustaf Dahl, Gothenburg, June 2018

Contents

| | | |
|----------|---|-----------|
| 1 | Acronyms | 1 |
| 2 | Introduction | 3 |
| 3 | Delimitations | 5 |
| 4 | Background & Theory | 7 |
| 4.1 | IoT and LPWAN | 7 |
| 4.1.1 | LPWAN | 8 |
| 4.1.2 | Sigfox - A short introduction | 9 |
| 4.1.2.1 | Sigfox - The technology | 10 |
| 4.2 | Batteries | 11 |
| 4.2.1 | Basic design | 11 |
| 4.2.2 | Lead-acid battery | 12 |
| 4.2.2.1 | Materials and chemical reactions | 12 |
| 4.2.2.2 | Self-discharge rate | 13 |
| 4.2.2.3 | Effects of temperature | 13 |
| 4.2.2.4 | Charging | 14 |
| 4.2.2.5 | Cycle life | 14 |
| 4.3 | Solar energy | 16 |
| 4.3.1 | The Sun and the Earth | 16 |
| 4.3.2 | Solar cell | 19 |
| 4.3.2.1 | Band gaps and p-n-junctions | 19 |
| 4.3.2.2 | Determining performance of a solar cell | 20 |
| 5 | Methods | 23 |
| 5.1 | Base station measurements and power consumption | 23 |
| 5.2 | Positioning | 26 |
| 5.2.1 | Angle of solar module | 31 |
| 5.3 | Choosing the right equipment | 32 |
| 5.3.1 | Solar Module | 32 |
| 5.3.2 | Battery | 34 |
| 5.3.2.1 | Type of battery | 34 |
| 5.3.2.2 | Battery capacity | 34 |
| 6 | Results | 37 |
| 6.1 | Autonomous above the Arctic circle | 37 |
| 6.2 | Universal technical parameters | 38 |
| 6.2.1 | Battery technology | 38 |
| 6.2.2 | Solar module | 39 |
| 6.2.3 | Power regulator | 39 |

| | |
|------------------------------|-----------|
| 7 Discussion | 41 |
| 7.1 Methods | 41 |
| 7.2 Improvements | 42 |
| 7.3 Final thoughts | 43 |
| Bibliography | 44 |

1

Acronyms

- *3G* - Third generation of wireless mobile telecommunications.
- *4G* - Forth generation of wireless mobile telecommunications.
- *Azimuth angle α* - The Sun's horizontal angle when above the horizon. Measured from the north (0°) counterclockwise.
- *Bandwidth* - The difference between the lower and upper frequency that a signal can be within. Measured in Hz.
- *BLE* - Bluetooth Low Energy, a short range communication technology.
- *D-BPSK* - Differential Binary Phase-Shift Keying, a type of PSK modulation that separates each phase by 180° .
- *Cardinal direction* - North, South, East and West.
- *Conduction band* - Electron band below the valence band, is essential to electrical conductivity together with the valence band.
- *ERP* - Effective Radiated Power [W], RF power.
- *Equatorial disc* - A disc intersecting the Earth with the equator as its edges.
- *GFSK-signals* - Gaussian Frequency-Shift Keying, a modulation type for RF signals.
- *GIS* - Geographical Information System, software used for collecting and analysing geographical data.
- *Group III* - Group of elements in the periodic system characterised by 3 electrons in the outermost shell.
- *Group IV* - Group of elements in the periodic system characterised by 5 electrons in the outermost shell.
- *GSM* - Global System for Mobile communication.
- *Insolation* - Solar irradiance over time ($W/m^2/h$)
- *IoT* - Internet of Things, umbrella term for a variety of communication technologies.
- *ISM band* - Industrial, Scientific and Medical radio bands. Frequency bands internationally reserved for these purposes.
- *June/December solstice* - When the sun is at a 90° angle to the Tropic of Cancer, Tropic of Capricorn respectively. Occurs approximately on June 21st, December 21st respectively.
- *LoRa* - LPWAN technology owned by Semtech.

- *LoRaWAN* - Communication protocol based on the LoRa technology.
- *LPWAN* - Low-Power Wide-Area Network
- *Meridian* - An imaginary line from the north pole to the south pole
- *MPP* - Maximum Power Point.
- *NASA* - National Aeronautics and Space Association
- *POWER* - Prediction Of Worldwide Energy Resources.
- *RF signals* - Radio Frequency signals, used to transmit information wireless between transmitters and receivers.
- *SLI battery* - Start, Lightning, Ignition battery. Used as starter batteries in cars, boats, RV's etc.
- *SMHI* - Swedish Meteorological and Hydro-logical Institute.
- *Solar elevation angle β* - The sun's vertical position in relation to the horizon. Horizon equals 0° .
- *Solar noon* - the highest solar elevation angle reached during the day.
- *Solar irradiance* - Power received per area unit (W/m^2).
- *Spring/autumn equinox* - When the sun is at a 90° angle to the equator. Occurs approximately on March 21st, September 21st respectively.
- *STC* - "Standard Test Conditions" for solar cells done with a cell temperature of $25^\circ C$, $1000W/m^2$ irradiance and air mass of 1.5 (AM1.5).
- *UNB* - Ultra Narrow Band, a type of frequency modulation.
- *Valence band* - The highest electron band, forms molecules with other atom's valence bands.
- *WiFi* - Wireless local area network.

2

Introduction

Internet of Things, or the more common acronym *IoT*, is sometimes referred to as a revolution [1]. The ability to allow electronic devices to communicate autonomously without the need of human interference opens up for so many possibilities that it justifies the use of the word "revolution" in the above sentence.

IoT applications are becoming increasingly common in manufacturing industries, transport and logistics, health care, homes and agriculture among many other fields. However, the various technologies enabling *things* to communicate rarely includes applications in remote and rural areas with no electrical grid connectivity. Despite the previous statement, there are many ways IoT could be utilised in remote areas such as to monitor environmental disorders and disasters, flora and fauna, crops and weather. Sectors with more of an economical interest such as lumber, mining and fishing could also benefit from IoT-solutions.

By employing the Sigfox *LPWAN* (Low-Power Wide-Area Network) technology, the *things* can start communicating wirelessly from these remote areas. To make this possible a system providing LPWAN coverage while operating in an area without electrical grid connectivity is needed. The aim of this project is to analyse the possibilities of designing a solution for powering a Sigfox SBS-T3-868 LPWAN base station north of the Arctic circle. A viable solution should fulfil the following requirements:

- Solar powered
- Low maintenance
- Easy to assemble and disassemble

The scope includes determining the necessary equipment and specifications that are crucial in keeping the system operational during the whole year, without being connected to the power grid or having the need for regular maintenance. The lack of sunlight and harsh weather conditions north of the Arctic circle presents a substantial challenge in meeting the above requirements. Therefore, a significant part of this project will be dedicated to researching the combination of solar cell performance and battery backup power.

By achieving the stated requirements, measuring and data gathering in remote areas would be simplified as there would be little need of human interference, apart from assembling. Designing with the intent of small size and lightweight would make the system *nomadic* - easy to move in order to supply coverage where coverage is needed.

The task and scope of this project has been established together with IoT Sweden, the owner or the Sigfox distribution licence in Sweden.

3

Delimitations

In order to limit the scope of this project the subjects and technologies that are described in this chapter will not be further studied and accounted for. Each of these subjects and technologies will be given a short description to why they will not be included further on in the project.

This project will focus on the standards and regulations of the Nordic countries and Europe. Application design and regulations for other regions will therefore be excluded in this report in order to limit the scope of the project.

In the report detailed information concerning the software and protocols of the Sigfox LPWAN technology will not be provided, since this project mainly concerns hardware.

Due to the fact that IoT Sweden only works with the Sigfox LPWAN technology this project will only focus on this IoT technology. This report will therefore not further describe the use of other IoT technologies such as GSM, 2G, 3G, 4G, 5G, WiFi, Bluetooth, ZigBee or other telecommunication technologies. Neither will it provide a detailed description of the technologies LoRa, LoRaWAN or other LPWAN technologies. These technologies will only be used as adversaries to compare with the Sigfox and LPWAN technology.

Due to the characteristics of different technology and materials used for battery cells this project will only cover batteries of the lead-acid type, Li-Ion will only be used as a comparison in one case. This is due to the fact that batteries like Li-Ion and NiCd either has a higher discharge rate, lacks the ability to operate efficiently in cold climates or are too costly.

The usage of wind turbines as a power source compliment to the solar modules will only be addressed in the discussion in Chapter 7, but it will not be further analysed in the report. Studies concerning the possibility for re-positioning solar modules by using servos or other rotation applications have not been done. This is due to the high-maintenance nature of systems with moving parts and the uncertainty concerning the lifespan.

This project will not involve any suggestions concerning the final design of a solar powered system for the Sigfox SBS-T3-868 base station. Chassis and assembly design will not be studied in this report neither will field tests and implementation tests be done due to time shortage and the size of the project.

The albedo effect have not been studied in this report, since no data was found showing its potential impact for the area investigated and since field test have not been conducted.

The theoretical background in this report will only supply the basic information needed to understand the technology used and to highlight the reasons for why certain key factors matter in the design, since the project corresponds to a bachelor thesis in the basic engineering education.

4

Background & Theory

In this chapter a basic background concerning IoT, LPWAN and Sigfox will be provided in order to give the background needed to understand how these technologies and networks operate. The theory concerning batteries, solar energy and solar modules will be explained in a more detailed way and will be used as reference to motivate and explain the choices made in the Method and Result chapters.

4.1 IoT and LPWAN

What is IoT and LPWAN? IoT translates into *Internet of Things* and includes all objects that can be connected to a network by using a type of information transmission technology. By connecting devices that gather information by monitoring and/or measuring specific changes in their immediate surroundings, data can be collected for the purpose of analysing the changes in those specific surroundings instantly or later on. The collected data can be used to analyse and evaluate changes in an illimitable amount of different fields. Examples of fields and areas where IoT is already helping with monitoring changes, evaluating efficiency and collecting data are; alarm systems, weather measurements, industrial flow control, emission levels in cities, seismological changes and smart cities. In Figure 4.1 a few examples of applications for a few different IoT technologies can be seen.

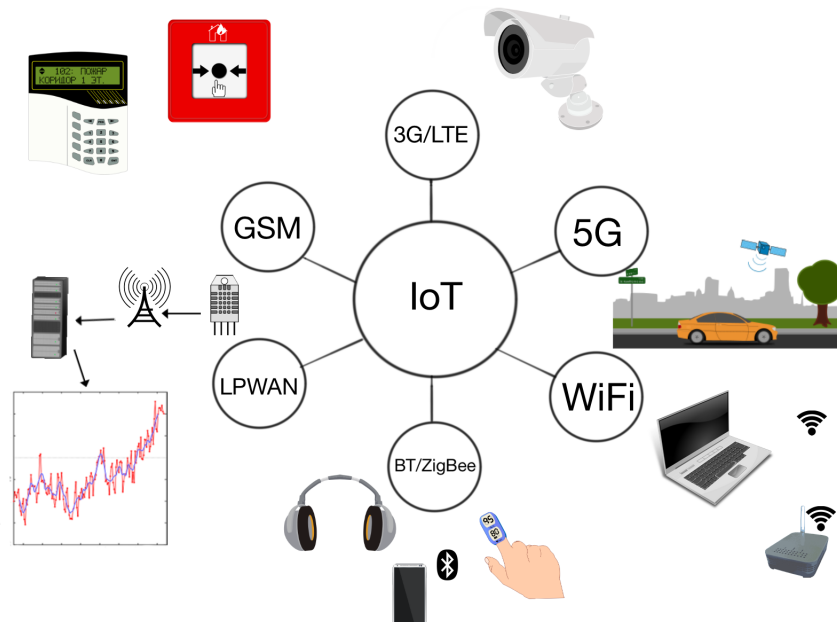


Figure 4.1: Some applications that utilises the major IoT technologies.

As mentioned, IoT is an umbrella term covering a wide variety of devices and technology that are used today for transmitting collected data. Some of these technologies are WiFi, GSM, 4G, 3G, Ethernet and LPWAN. All of these technologies are used for different fields and needs but this project will only cover LPWAN.

4.1.1 LPWAN

Low Power Wide Area Network (LPWAN) is a technology used for transmitting small data packages over long distances and it is suitable for a variety of IoT and M2M (Machine to Machine) applications. Compared to other IoT technology, LPWAN is both energy efficient and long range, due to the use of low carrier frequency (explained in Subsection 4.1.2.1), which makes it ideal for wireless connection of gauges and sensors in hard to reach and exposed areas [3]. The technology allows an extended battery life and many devices can operate for up to 10 years on the same battery, which drastically lowers the maintenance time and cost for each sensor.

Each LPWAN endpoint device connects to a radio base station, which decodes and relays the data package to the back-end servers where the data can be stored for the user to view and analyse when needed, as explained in Figure 4.2.

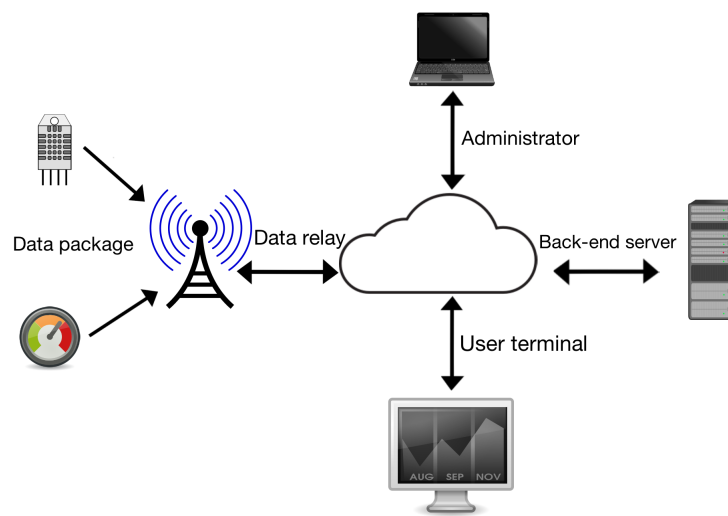


Figure 4.2: A rough sketch of a LPWAN communications network.

Each IoT technology offers their own exclusive possibilities and limits, which makes them a good choice for different fields of applications. Technologies such as *BLE* (Bluetooth Low Energy) has a maximum range of 30 meters and Zigbee offers a coverage of 100 meters while the LPWAN technology not only has an extended battery life but it also gives a much larger coverage, with up to 100 km in some cases [2], [4]. The trade-off however is that the data package size that can be transferred with the LPWAN technology is very limited while Bluetooth and Zigbee allow for much bigger data packages. The same applies for GSM technology, which is long range and can deliver larger data packages but has a higher energy consumption while operating and also requires a bulky sim card.

In Figure 4.3, the performance and key factors of some of the most used IoT technologies can be viewed to further explain their characteristics.

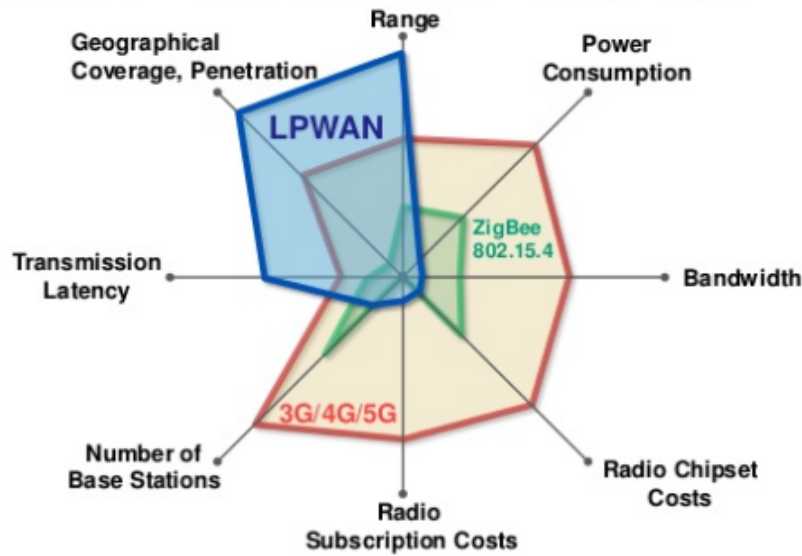


Figure 4.3: The different characteristics and performance of IoT technologies. Used with permission of Techplayon.com, copyright by Techplayon.com.

The LPWAN networks are built to operate within the license free frequencies contained in the regulated *ISM* (Industrial, Scientific and Medical) band. The ISM bands are reserved for the transmission of RF signals used in industrial, scientific and medical applications and therefore exclude telecommunication from its frequency bands [5]. The frequencies that make up the ISM band differ between regions and countries and they are mostly used for short range devices (Bluetooth, Zigbee), but in Europe long range devices are allowed to operate within the frequencies 863MHz to 870MHz [6]. The frequencies that make up this band are divided into sub-bands that allow different duty-cycles and *ERP* (Effective Radiated Power) for each radio device[9]. Due to the regulations of the ISM-bands, the radio devices used in the LPWAN endpoint applications are only allowed to send a maximum sized data package at a certain bitrate during a limited time window. This means that applications that communicates via a LPWAN network do not have the possibility to report changes in sensors and gauges in real time, since the regulations permit the endpoint devices from transmitting its collected data all the time. Hence, LPWAN is not considered to be an option for time critical measurements but rather for collecting data over a longer time spectrum [8].

There are multiple companies developing their own LPWAN networks today, the biggest ones are Sigfox and *LoRaWAN*. The technology is based around the same principles, using the free ISM-bands for long range communication and keeping the endpoint devices as energy efficient as possible. However, the different companies have developed their own unique business models and technologies to create coverage and usability for their LPWAN network. This report only focuses on the technology developed by Sigfox.

4.1.2 Sigfox - A short introduction

Sigfox is a French company, based in Toulouse, that has developed their own LPWAN technology, protocol and standard. Since the start in 2010 the network capacity of the company has grown to include IoT solutions in 45 countries globally [10]. Sigfox wants to speed up the development and implementation of IoT and M2M solutions on a global scale and therefore their focus is to develop and create a global network coverage for LPWAN devices, as well as

developing affordable LPWAN modems that are easy to implement and merge with the users devices [10], [11].

The business model used by Sigfox focuses on creating an affordable solution that is easily accessible and easy to implement for the user [10]. The endpoint modem, used for connecting a device to a radio base station, is therefore relatively cheap in comparison to other LPWAN chip manufacturers, since Sigfox believes that the cheaper and easier it is for a customer to implement an IoT solution, the faster the development of IoT will progress [13]. In contrast to the Semtech owned *LoRa*, Sigfox have teamed up with a variety of chip manufacturers that build and develop the modems used in the endpoints, lowering the cost for each modem and therefore making them more easily attainable for the user. Similar to regular telecommunications companies Sigfox owns the networks and the gateways together with their licensed partners while the user pays a subscription fee for the Sigfox unit they use [11].

Compared to the subscription free- and open source LoRa networks, where the network coverage is made up of gateways managed by private companies or individuals, the Sigfox network is managed by companies that have been chosen by Sigfox to build and supply a region with their LPWAN network coverage. In Sweden the company in charge of the establishment and maintenance of the Sigfox LPWAN network is *IoT Sweden*, based in Stockholm.

4.1.2.1 Sigfox - The technology

This subsection will provide more information concerning the technology used by Sigfox and how the networks operate. Since this project is oriented towards the radio base station rather than a device using a Sigfox modem, this subsection will in general terms describe how the transmission between the endpoint devices, the base station and back end servers works.

As explained in Figure 4.2, each endpoint device using a Sigfox modem transmits its collected data to a radio base station. Each message can contain a data package of maximum 12 bytes. The base station decodes the data package and transmits it on to the Sigfox back-end servers, where the data is processed and then sent to the correct user who can save the data for further analysis.

The Sigfox network system is built upon *cooperative reception*, which means that an endpoint device using a Sigfox modem connects itself to any base station nearby and a single device can connect to multiple base stations at the same time [14]. This is called *spatial diversity* and it is used to guarantee a higher success rate for the delivery of each message.

A Sigfox modem communicates with each base station via RF-technology, transmitting over the free ISM-bands. The ISM-frequencies used by Sigfox in Europe are in the bandwidth 868 MHz to 868.6 MHz and as explained in subsection 4.1.1, each ISM-band has their own restrictions [14]. The regulations for each sub-band in the ISM-band can be found in the Bibliography chapter, but for the 868 MHz to 868.6 MHz band the following limitations are set [6]:

- Duty cycle = 1%
- ERP = 25mW

These regulations permits the endpoint device from sending data more than once every 10 minutes, which totals in 6 messages per hour or a maximum of 140 messages a day. Due to these characteristics, the Sigfox LPWAN system is not reliable for monitoring some time critical changes but on the other hand it also helps the system to conserve energy, since it is not

possible to send data without a time gap of 10 minutes [14].

To be able to design a network that can communicate over longer distances while also prioritising small energy usage, Sigfox use UNB (Ultra Narrow Band) and *D-BPSK* (Differential Binary Phase-Shift Keying) modulation for communication between the endpoint modem and the base station [7].

The advantages of UNB and D-BPSK modulation are many for this specific type of network and their characteristics are one of crucial components of the system design.

D-BPSK is a simple modulation technique that lacks the possibility to send larger amount of data, but it is easy to implement in terms of circuitry, which lowers both costs and size for each receiving and transmitting module [8]. Another aspect of D-BPSK is that it is much easier for a receiver to decode, since the modulation format is less sensitive to noise compared to higher-order formats [7].

The use of UNB-modulation enables the network to work over longer distances and lowers the risk of colliding messages, as compared to conventional *GFSK* (Gaussian Frequency Shift-Keying) signals [15]. The UNB-technology enables an efficient use of the entire band-width and in comparison to other modulation technologies, UNB do not make use of the side bands.

The key factor of the Sigfox networks are the radio base station. To be able to design a network that is easy for a consumer to connect their device to the Sigfox system is based around a more complex base station [8]. The base station usually do not have the need to be power efficient or easy to integrate, since the base stations are owned by a licensed company and therefore not public. All the Sigfox base stations relays the information gathered from the endpoint devices to the Sigfox back-end servers, and finally to the correct user. There are multiple options for the base station to establish communication with the back-end. The base station used for this project, the Sigfox SBS-T3-868, allows for communication via either 3G/4G, Ethernet or satellite.

4.2 Batteries

A battery is a unit used to store energy that is to be consumed later on. There are two types of batteries, primary and secondary types. A battery of the primary type is a unit that is used only once and then disposed of, meaning that when the energy stored in its cell is depleted the unit is sorted as garbage of the correct type [16]. Typical batteries of the primary type are AA, AAA and button cells. A battery of the secondary type is a unit that is designed to be reused and recharged multiple times before its disposal. This type of battery is also known as an accumulator, since it is used to accumulate energy over and over [16]. Typical batteries of the secondary/accumulator type are used in vehicles, power tools and mobile phones. A secondary type battery can operate in three different stages; the charging state, the discharge state and the standby state.

The scope of this report does not include batteries of the primary type and therefore they will not be further addressed in the report.

4.2.1 Basic design

A battery package is made up by an array of battery cells. The number of cells in a battery package depends on the application the battery is supposed to power, more cells are needed for powering an application that needs a higher voltage and vice versa. The number of cells in a battery package affects the total size, weight, cost and performance of the battery package [17]. Cells can be designed in different ways, with different materials and properties but they usually contain the same four main components:

two electrodes, the separator in between them and the surrounding electrolyte [16][18].

The two electrodes are the positive anode and the negative cathode, which are both made of different materials. The electrolyte is a ionised chemical composition that can be either liquid or solid. The electrolyte surrounds the two electrodes inside the battery package or battery cell and connects the two electrodes. Because of the chemical characteristics of the electrolyte it can conduct charges between the anode and the cathode, which closes the circuit, making it possible for negative and positive charges to travel between the two electrodes [18], [19].

The separator is placed between the two electrodes to provide insulation between the positive and the negative electrode but also to provide an ionic flow inside the battery cell [19]. There are many different types of separators that can enhance the battery performance, however this will not be further discussed in this report.

There are both solid and liquid types of electrolyte, but for applications requiring higher output voltages liquid electrolyte is the mostly used [19]. The scope of this report limits the choice of battery technology and will include only those of the liquid electrolyte type and further information and background concerning the other types of electrolytes or more detailed description of the chemical composition of the liquid electrolytes will not be made.

Secondary type batteries comes in different shapes and sizes depending on the application it is supposed to power. By choosing the materials the cell components are made of it is possible to alter the characteristics of the battery. All battery types stores energy chemically and when connected to a load the chemically stored energy is converted into electrical energy, that can be used to power the wanted application [16], [17]. Performance in different fields will vary depending on the conductivity of the materials used, how strong and durable the material are or how they are effected by low or high temperatures etc. Costs will increase or decrease depending of how rare the material is and how difficult it is to process.

Due to the low temperatures that occur in the Nordic countries during winter, the only suitable battery technology for this project is of the lead-acid type. Why this is the case will be further explained in section 4.2.2. Because of the inability to work in low temperatures and/or without regular maintenance other battery technologies will not be further discussed in this report.

4.2.2 Lead-acid battery

In this section, the key parameters of the lead-acid battery will be explained. The functionality of the cells as well as the characteristics of the materials used will be covered in order to provide insight into the positive and negative aspects of a lead-acid battery.

4.2.2.1 Materials and chemical reactions

In the charging state the lead-acid cell consists of the lead dioxide (PbO_2) anode, the lead (Pb) cathode and the sulphuric acid (H_2SO_4) electrolyte [19]. In the discharge state the components characteristics changes due to the chemical reaction and both the anode and cathode consumes the sulphate ions and converts into lead sulphate ($PbSO_4$). When discharging, the concentration of sulphuric acid (H_2SO_4) in the electrolyte is reduced and as the battery becomes fully discharged the electrolyte has been reduced to contain almost only water [19].

When charged, the concentration of sulphuric acid (H_2SO_4) in the electrolyte rises. The potential of a single lead-acid battery cell is effected by operating temperature, humidity and the state of the battery but it can be determined that the nominal voltage of a single lead-acid battery cell is 2 Volt [19].

4.2.2.2 Self-discharge rate

A common factor for all types of batteries is the self-discharge phenomenon. When there is no load powered by the battery, the cell acts like an open circuit and due to chemical reactions in the cell it loses a certain amount of energy over time. This is called the self-discharge rate [16], [19].

The self-discharge of the lead-acid battery is caused by the difference in voltage potentials of the anode and the cathode. When the battery is in an open circuit state and no current passes through the electrodes, amounts of H_2 and O_2 evolve due to the chemical reactions in the cell. As the amount of H_2 and O_2 rises, pressure starts to build up inside the battery. This pressure has to be passed out through the release valve on the battery package in order to maintain a correct pressure level inside the battery package. These gases contain energy that has escaped from the active materials in the battery package, which the battery loses when they are released through the release valve.

This means that the battery will lose stored energy over time when it is not being either charged or discharging its energy over a load [19]. Experiments that have been done on lead-acid batteries suggest that they have a self-discharge rate of 2% in one month time [19]. This value is general, since multiple factors such as, temperature, electrolyte formulation, and grid alloy composition effects the rate differently.

4.2.2.3 Effects of temperature

Many parameters in a battery are temperature sensitive and the characteristics of the battery cells may change as a rise or fall in the surrounding temperature occurs. The air temperature affects the temperature of the electrolyte inside the battery package and depending on the temperature of the electrolyte the characteristics of the battery may change [20]. Some of the lead-acid parameters that are affected by changes in temperature are [19], [20]:

- Charging efficiency.
- Self-discharge rate.
- Battery resistance.
- Energy capacity.
- Cell durability.

All batteries, no matter the technology, allow for a minimum and maximum electrolyte temperature. When the electrolyte gets warmer or colder than these specific restrictions the battery loses the possibility to charge properly and the self-discharge rate will change depending on if the electrolyte is hot or cold [20].

Lead-acid and Li-Ion batteries have widely different material characteristics which makes the two technologies better for different fields of use. However, the Li-Ion battery does not work well with cold temperatures, as it can not be charged when the electrolyte reaches a temperature of 0°C [20], [19]. The lead-acid technology on the other hand allows the battery to be charged even when the temperature of the electrolyte is -20°C . This makes the lead-acid technology the only real choice for applications that are supposed to operate in areas with cold weather.

The lead-acid battery's ability to operate under harsher circumstances makes it more suitable as a battery in a power source backup system or as a starter battery in a car. However, as mentioned in Subsection 4.2.2.1 the electrolyte of the lead-acid battery becomes closer to water as the amount of energy stored in the cell gets lower, which then means that when the energy source is depleted and the electrolyte is close to containing only water, it freezes at 0°C . This

will lead to complete breakdown of the battery and it then has to be replaced. It is therefore very important that a lead-acid battery is not left discharged in cold temperatures.

4.2.2.4 Charging

When a lead-acid battery is being charged, the concentration of the sulphuric acid electrolyte changes from low to high concentration, as explained in Subsection 4.2.2.1. The sulphate ions then moves from solid to liquid form and while doing so, redistribution of the active material can occur, causing the active material to become less chemically active [19]. This is called *physical degradation* and it is the reason why all batteries have a limited life time/charging cycles. *Physical degradation* can be minimised by making sure that the battery is charged properly to maximise the amount of charging cycles that can be used.

In order to avoid gassing and *physical degradation*, the amount of charging current needs to be regulated. One way of doing this is to use a battery charger that regulates the charging current depending on the amount of energy currently stored in the battery.

There is a variety of ways and standards used to charge batteries but this report will only focus on the charging methods used for stationary lead-acid batteries of the deep-cycle type which includes two methods: the *constant-current charge followed by constant-voltage charge* and *float charging* [19]. When charging a battery using these two charging principles, the charging process goes through three stages: Bulk, Absorption and Float [21], [19].

During the first stage (Bulk) the charger applies a constant and high charging current in order to rapidly charge the battery to 80-90% of its total capacity. The charging current is held constant against the rising internal resistance in order to raise the voltage level of the battery.

In the second stage (Absorption) the charger raises the charging voltage and lowers the charging current, keeping the charging voltage at a constant level to avoid gassing and minimising the risk for *physical degradation*. As the internal resistance rises and the voltage is held constant the current is lowered. This is done until the battery is charged to 100% of its capacity and the third stage is entered when the battery is down to approximately 98%.

During the third stage (Float) the charger keeps a constant voltage level, floating the battery charge between 98-100%.

4.2.2.5 Cycle life

All batteries have a limited number of charging cycles due to the material characteristics of the components in the battery. Charging cycles is a term used to provide a rough measurement of the expected lifetime of a battery. The amount of charging cycles a battery can supply depends on the amount of energy that is drawn from the battery before being charged back to full capacity each time. The measurement of charging cycles is therefore dependent on continuity and the fact that the user knows how much of the energy capacity they will draw from the battery with each use. It is therefore hard to tell what to expect in terms of battery lifetime without knowing how much energy that will be drawn from the battery continuously.

There are a variety of lead-acid batteries with different performances available on the market today.

One type that is widely used for stationary backup power applications is the *deep-cycle* type. The deep-cycle type allows for a greater use of the total battery capacity, by allowing a discharge rate of around 80% before risking to cause damage to the battery cells. A battery of the deep-

cycle type also allows for more charging cycles and smaller discharge rates. This is done by making the cell-plates thicker, hence making the deep-cycle batteries both heavier and more expensive [19].

Table 4.1 shows the difference in the amount of cycles a regular SLI battery can withstand in comparison to a battery of the Deep-cycle type. Depth of discharge is a measurement of how much energy that has been drained from the total capacity of the battery when fully charged and the table shows the correlation between depth of discharge and the number of charging cycles.

Table 4.1: Correlation between number of charging cycles and depth of discharge, based on Table 1.13 in [19]

| Depth of discharge: | SLI battery | Deep-cycle battery |
|---------------------|----------------|--------------------|
| 100%: | 12-15 cycles | 150-200 cycles |
| 50%: | 100-120 cycles | 400-500 cycles |
| 30%: | 130-150 cycles | 1000+ cycles |

4.3 Solar energy

Beginning with the Sun and how energy is generated, this section explains the basic reasoning for the varying seasons of the Earth and the limitations of implementing photovoltaics in the Nordics. Furthermore, the process of converting the Sun's electromagnetic radiation to electricity is briefly explained, as well as the key factors affecting the efficiency and therefore the performance.

4.3.1 The Sun and the Earth

By the process of fusion in the core of the Sun, hydrogen nuclei are transformed into a helium nucleus plus energy. The amount of energy is determined by the difference in mass of the hydrogen nucleus and the helium nuclei where the hydrogen is heavier, hence energy is released [22]. The relation between mass and energy is described by the mass-energy equivalence in Equation 4.1, where it is easy to see that a small mass contains a large amount of energy due to the mathematical relation including the multiplication with the *speed of light* squared.

$$E = mc^2 \quad (4.1)$$

Eventually the energy, partly consisting of photons, is transmitted from the surface of the Sun. The transmitted photons have lost a lot of energy on its way from the Sun's core to leaving its surface. The energy level of the photons represents the *solar spectrum* which extends from approximately 300nm to 3000nm [23]. It includes visible light as well as some IR-radiation and UV-radiation as seen in Figure 4.4. Upon reaching the surface of the Earth, the *solar irradiance* can be approximated at a power of $1000\text{W}/\text{m}^2$ at sea level. However, there are sizeable seasonal and position based variations and since the scope of this thesis is focused on the Nordic countries, that will also be the focus in this section. The first step is figuring out why the seasons vary to such an extent in the Nordic countries and the reason for the cold climate in the region.

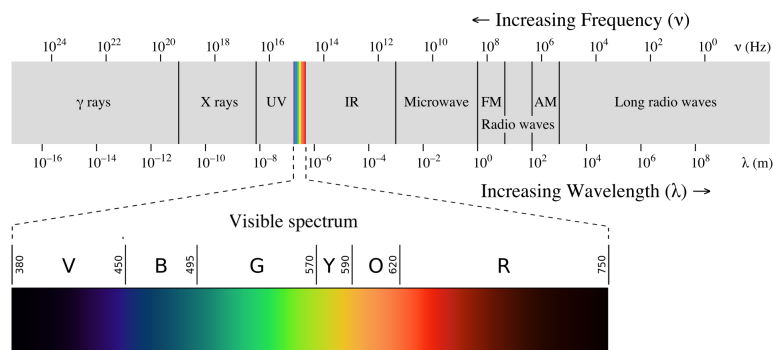


Figure 4.4: The electromagnetic spectrum with the wavelengths corresponding to visible light emphasised. Image courtesy of [24]

The Earth has an axial tilt of approximately 23.44° which means its rotational axis does not align with its orbital axis and the difference is the angle. This is what causes the seasons of the Earth. Focusing on the Northern Hemisphere, during the *June solstice* the axial tilt causes the Northern Hemisphere to "lean in" 23.44° towards the Sun resulting in 24 hour daylight above the latitudinal line at approximately 66.56° , called the arctic circle, during this time. On the contrary, during the *December solstice* the Northern Hemisphere faces 23.44° away from the Sun causing total darkness in the same region [25].

As can be seen in Figure 4.5, illustrating the Earth's orbit and axial tilt, sunlight in the Northern Hemisphere is lesser from the autumn equinox to the spring equinox with peak darkness at the December solstice as a result from the axial tilt. Hence the varying seasons.

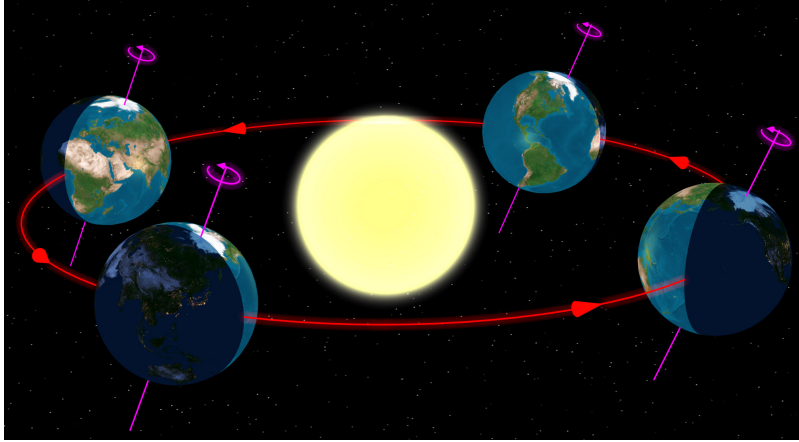


Figure 4.5: The Earth's orbit seen from north, showing the spring/autumn equinoxes as well as the June/December solstices. Picture from Wikimedia commons, CC0 1.0 Universal Public Domain Dedication. Available: https://commons.wikimedia.org/wiki/File:North_season.jpg

Harvesting the solar irradiance (W/m^2) to the largest extent possible is the essence of photovoltaics. A common term when discussing the power generated by a photovoltaic system is *insolation*, which is the measurement of the power per unit area from the Sun's electromagnetic radiation over time. The insolation is largely dependent on the angle of the incoming solar irradiance, when the Sun's rays are normal to the Earth's ground the insolation is stronger, as illustrated in chapter 2 of [30]. This is one of the reasons the equator has a warmer climate than the Nordics. This phenomena is illustrated in Figure 4.6, the solar irradiance is spread out over a larger area when the angle decreases or increases from being normal (90°) to the Earth's ground.

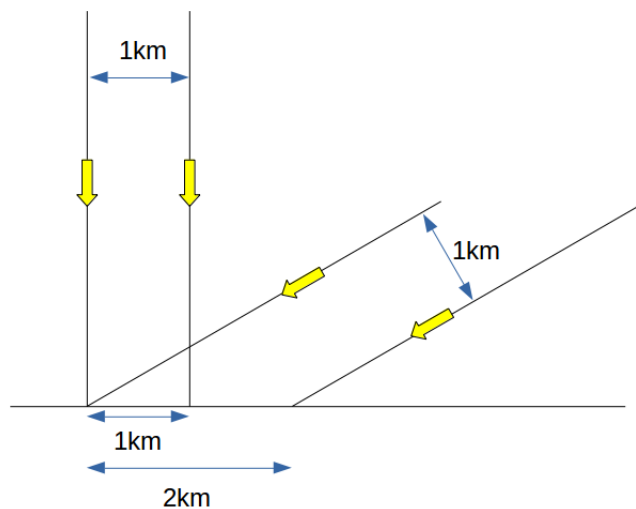


Figure 4.6: The difference of insolation depending on the angle of the sunlight. Illustrated are incoming solar irradiance at 90° - and 30° angles.

A larger perspective of the same concept can be seen in Figure 4.7, displaying the conditions during an equinox, when the *equatorial disc* is parallel to the Sun's rays. The same concept is

applicable for the *Tropic of Cancer* and *Tropic of Capricorn* during the June- and December solstice. However north of approximately 23.44° latitude the Sun's rays hit the Earth at a gradually lower angle. Using the example in Section 5.2, Figure 5.7 it can be seen that the highest mean solar elevation angle measured in the Tarfala area (67.9° latitude) is 45.1° . This greatly limits the amount of energy potentially harvested from the Sun in the Nordics.

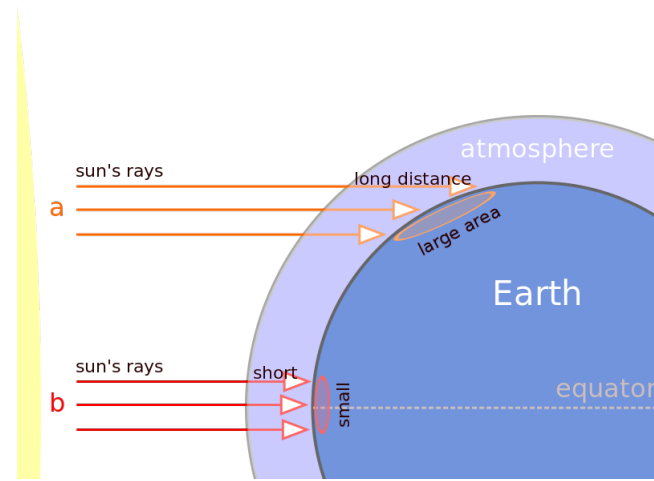


Figure 4.7: Variation of insolation in the Northern Hemisphere during an equinox. Image courtesy of [26].

To produce a number representing the total irradiance as close to the earths as possible, the *diffuse irradiance* has to be accounted for. When the radiation enters the atmosphere, some of it becomes scattered by the small particles it hits in the atmosphere. This means that apart from the direct irradiance, small amounts of radiation are reflected from particles in the atmosphere - some of it reaching the surface of the Earth. This is called diffuse irradiance.

In cloudy areas, like the Nordic countries, this proves to be a substantial addition to the direct irradiance. Therefore the total irradiance G_{TOT} is the sum of the direct irradiance G_{DIRECT} and the diffuse irradiance $G_{DIFFUSE}$ as seen in Equation 4.2

$$G_{TOT} = G_{DIRECT} + G_{DIFFUSE} \quad (4.2)$$

The concept of diffuse- and total irradiance is explained in chapter 2 of [30].

4.3.2 Solar cell

The process of converting light into electricity is called photovoltaics, which involves the theory that forms the basis of the functionality of solar cells. The solar cell consists of a semiconducting material that changes its electrical properties when exposed to electromagnetic radiation. A semiconducting material is generally chosen to absorb as much as possible of the electromagnetic radiation from the chosen source of light. In the case of solar power, solar cells made of monocrystalline *silicon* (*Si*) has favourable characteristics when exposed to the solar spectrum¹, which makes it a very common semiconducting material in photovoltaic applications [30].

This section aims to provide a basic understanding of which factors affect the performance of a solar cell, with emphasis on the benefits and limitations experienced in the Nordics.

4.3.2.1 Band gaps and p-n-junctions

The solar cell is made up of a thin layer of a semiconducting material spread out over an area. The physical as well as the electrical properties are determined by the material used - silicon is common but also compounds such as cadmium telluride and gallium arsenide [30]. Ignoring the physical aspect and instead focusing on the electricity generating properties, the important difference can be traced to the varying distance from the *valence band* to the *conduction band* in the element or compound, this distance is called the *band gap*. To properly understand how electricity is generated using photovoltaics, some basic understanding of band gaps and p-n-junctions are required. Further on in this chapter, all examples are based on monocrystalline silicon solar cell.

The band gap is the measure of energy difference between the valence band and conduction band in an atom [30]. In other words it determines the increase in energy required for an electron to excite from its current orbit in the valence band to orbiting in the conduction band. A larger band gap generally provides insulating properties in a material whereas a smaller band gap generally provides the opposite. The energy increase in the case of solar cells comes from exposing the semiconducting material to sunlight where the photons must have an energy level corresponding to the band gap energy level in order to excite an electron from the valence band to the conduction band [30]. This is illustrated in Figure 4.8 where the longer wavelength radiation provides too little energy, hence not correlating to the band gap energy level of silicon $\sim 1.1eV$. What is also visible is that the semiconductor is not able to convert all of the high energy signals to electricity, this is also a limitation of the material where the excess energy is converted to heat.

¹Evaluating how favourable a specific material is in PV-applications requires knowledge of direct- and indirect gaps. Silicon possesses an indirect gap which implies poor light absorption [27], however this problem is solved in solar cells by using a thick silicon-layer which reduces the amount of low-energy radiation passing through the cell without being absorbed.

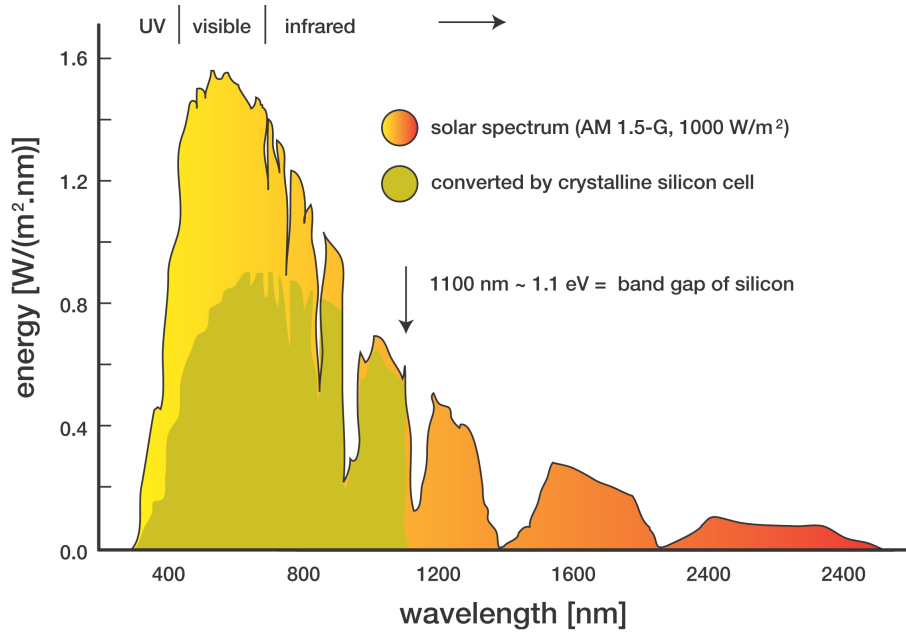


Figure 4.8: The different energy levels of the solar radiation on the Earth with regards to wavelength. Shaded area is the amount energy potentially absorbed by a crystalline silicon cell to create electricity. Image courtesy of [28].

A crystalline silicon solar cell consists of two semiconducting materials - one layer of *p-doped* silicon and one *n-doped* silicon. The *p-doped* layer consists of silicon embedded with a **Group III** dopant, commonly boron (B) which has three valence electrons. The boron atom bonds with three of the silicon valence electrons and leaves one *hole*, hence the layer being a positive charge carrier. The *n-doped* layer can be explained in the same manner but is embedded with a **Group IV** dopant, commonly phosphorus (P) which has five valence electrons, therefore this layer will be a negative charge carrier [30].

This layering of materials results in a semiconducting *p-n junction* where electron carriers move from the n-type region to the p-type region when exposed to light corresponding to the band gap energy. This flow of electric charge is called the generated current, I_G , and when connected to a load it produces a voltage.

4.3.2.2 Determining performance of a solar cell

While the theory presented in Section 4.3.2.1 concerns the functionality of a cell, a single cell is seldom used in practice. A solar module (panel) is the result of several cells connected in series and parallel to reach a power level that matches the consumption of the load.

The open circuit voltage V_{OCG} and the short circuit current I_{SCG} represents the highest voltage and current respectively, that is achievable in a solar module. These values are used when calculating the relation between the generated voltage V_G and current I_G . This relation is described in Equation 4.3, [29]

$$I_G = I_{SCG} \left(1 - \exp \frac{V_G - V_{OCG} + I_{SCG} R_{SG}}{N_s V_t} \right), \quad (4.3)$$

where N_s is the number of cells in series of the module, and V_t is the thermal voltage. The relation in equation 4.3 provides a function where size of the module (N_s), electrical losses (R_{SG}), solar irradiance (I_{SCG}) and temperature of the cell (V_{OCG} and V_t) are all considered. However, a few assumptions have been made to reach this relation, for a thorough description see [29]. Below is a brief overview of the assumptions:

- In the case of cells connected in parallel, the effects of the parallel resistance R_P is negligible.
- The series resistance R_S is not affected by irradiance or temperature.
- The short circuit current I_{SCG} is exclusively and linearly dependent on the solar irradiance.
- The open circuit voltage V_{OCG} is exclusively dependent on the cell temperature, with a reduction rate of $-0.0023V/^\circ C$.

In normal operating conditions these assumptions amount to a small error ($< 1\%$) that is commonly seen as negligible.

While maintaining high performance from a battery in the cold temperatures faced in the Nordics will prove to be a challenge, most solar cells show improved performance in cold temperatures. The reason for this phenomena can be traced to the increased density of charge carriers in the p-n-junction that is a result from the decreased oscillation of particles when the temperature drops. This is a simplistic way of explaining the temperature dependency and a more detailed description can be found in chapter 3 of [30]. In Figure 4.9 the effects of temperature is illustrated, clearly showing an increase in power during colder conditions.

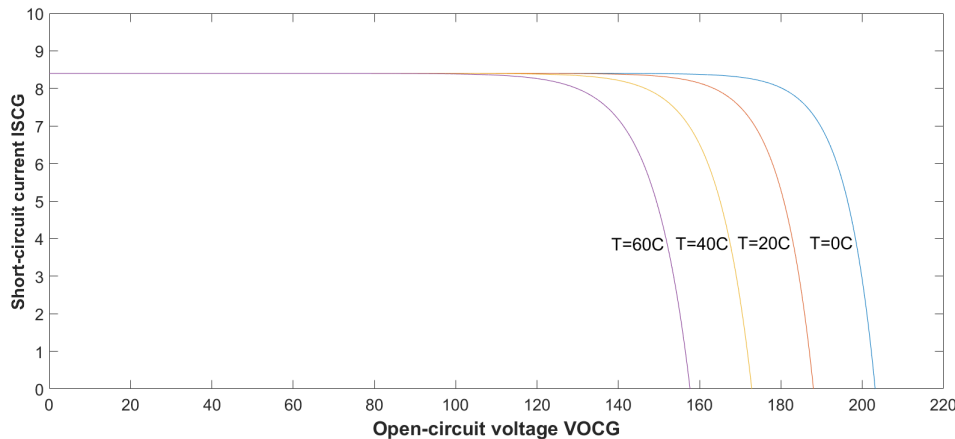


Figure 4.9: Temperature heavily affects the open-circuit voltage, increasing the power as the temperature decreases. Graph based on an example from [29] which represents a larger sized PV array.

It can be intuitively understood that an increase in energy of the solar irradiance leads to an increase in generated power from the solar cell. This relation is linear due to the assumption regarding I_{SCG} made above. This is illustrated in Figure 4.10 where it can be seen that the irradiance has a notable effect on the short-circuit current. As explained Section 4.3.2.1, a boost in insolation creates more electron-hole pairs, thus increasing the flow of electric charge which is synonymous with electric current.

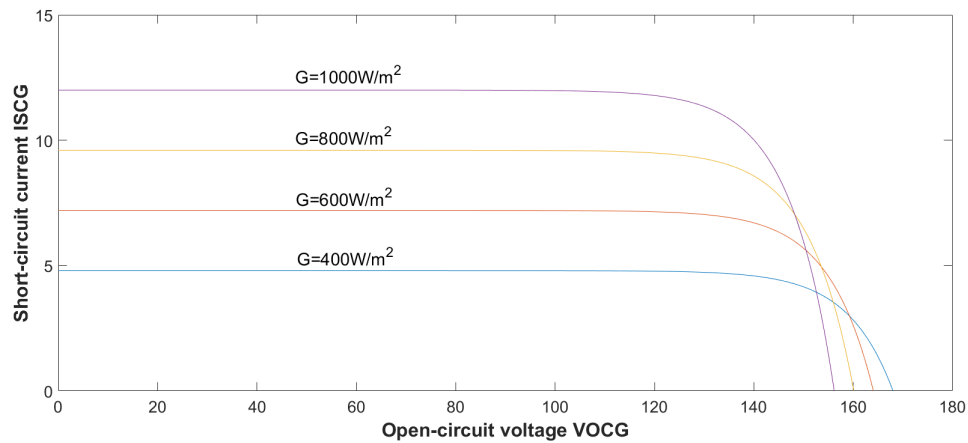


Figure 4.10: Solar irradiance mainly affects the short-circuit current. The open-circuit voltage is also affected, although to a much smaller extent, hence to the dependency statement above. The power increases as the irradiance increases. Graph based on an example from [29] which represents a larger sized PV array.

Figures 4.9 and 4.10 illustrates that cold and sunny environments are desirable for photovoltaic systems. The preferable point of operation is located at the "knee" of the plots and is commonly referred to as *MPP*, or Maximum Power Point.

Figure 4.9 and 4.10 was produced using MATLAB with the equations derived in chapter 2 and 3 of [29].

5

Methods

To produce a result, the first step is to determine the power consumption of the Sigfox SBS-T3-868 base station. Secondly, the conditions for a specific location need to be studied. This will assist in optimising the system powering the base station. Towards the end of this chapter, the necessary data for calculating a result will be presented, along with the appropriate solar cell- and battery technologies.

5.1 Base station measurements and power consumption

In order to establish the size of the solar module and the needed battery capacity, the total power consumed by the base station has to be measured. As seen in Table 5.1, the Sigfox SBS-T3-868 base station ideally uses 12 VDC (minimum 10 VDC, maximum 14 VDC) for supply voltage and consumes at maximum 6 A.

The power consumed by the Sigfox SBS-T3-868 base station while operating in Rx and Tx-mode can be found in the datasheet and are presented in Table 5.1.

Table 5.1: The consumption parameters for the Sigfox SBS-T3-868 base station [31].

| Parameters | Value Min | Value Max |
|--------------------|-----------|-----------|
| POWER CONSUMPTION: | | |
| Rx mode: | 30 W | 30 W |
| Tx mode: | 60 W | 60 W |
| POWER SUPPLY: | | |
| Supply voltage: | 10 V | 14 V |
| Current: | | 6 A |

The SBS-T3-868 base station enters Rx-mode when it receives a message and then starts decoding the data package from an endpoint device, while it enters Tx mode when transmitting the acquired data package to the back-end server. The base station always transmits a received data package, which means that it always enters the Tx mode after the Rx mode has been terminated [14].

Since these parameters only represent a general indication of the expected amount of power consumed by the Sigfox SBS-T3-868, a series of measurements was conducted in order to determine the total amount of power consumed over a period of time. To do this we used a *SEM 16+* standby energy-monitor from NZR, a company that develops measurement devices for multiple areas of use, see Figure 5.1.



Figure 5.1: A SEM 16+, courtesy of NZR.

The SEM 16+ measures a number of parameters over time and the device is used mostly to determine the long time energy consumption of a device or application. The Sigfox SBS-T3-868 base station was connected to the SEM 16+ and operated for 72 hours while measuring. An additional measurement was done over the course of one hour as well. These measurements are presented in Table 5.2. An additional consumption test was also done, measuring the total energy consumption of the SBS-T3-868 over 51 hours. The 51 hour test was an identical match to the 72 hour test shown in Table 5.2, therefore making the 72 hour test more valid.

Table 5.2: The measured energy consumption parameters for the Sigfox SBS-T3-868 base station.

| Parameters | Value |
|------------------|-----------|
| 72 HOURS: | |
| Max power: | 23,4 W |
| Min power: | 13,6 W |
| Total power: | 1,259 kWh |
| 1 HOUR: | |
| Max power: | 18,3 W |
| Min power: | 16,9 W |
| Total power: | 0,017 kWh |

The total energy consumption of the base station is defined by the time it spends in each of the three operating modes (Rx, Tx and standby-mode) and the energy consumption for each of these cases.

While analysing the test result, we discovered that almost none of the measured data in Table 5.2 matched the power consumption parameters listed in Table 5.1. However the data sheet for the Sigfox SBS-T3-868 does not reveal or further explain much about how much time the base station spends in each mode or what the overall power consumption of the unit is.

It is also hard to tell how accurate the measured power consumption in Table 5.2 is, since it has proved hard to measure the amount of network traffic that has been going through the measured base station and since much of the information needed to perform an accurate calculation is missing from the Sigfox SBS-T3-868 data sheet.

Sigfox have not conducted measurements of a Sigfox SBS-T3-868 base station that are publicly available, nor have they provided extra technical data concerning the time the base station spends in each mode.

Due to these difficulties, the test results in Table 5.2 will be considered as the power consumption of the base station. This number is acquired by dividing the *Total power* by the length of the test, this calculation yields $\sim 17.3W$. However, it is advisable to perform a power consumption test of the Sigfox SBS-T3-868 base station when operating in a normal trafficked area in order to optimise the system.

By using Equation 5.1 the amount of current the base station consumes during ideal circumstances can be calculated. This also translates to the total current consumption of one hour, which also can be used to calculate the total current consumption during one day.

$$I = \frac{Wh}{V} = 1.4Ah \rightarrow I \times 24 = 33.6Ah \quad (5.1)$$

The parameters for Equation 5.1 are:

- Wh - The amount of work during one hour, in this case 17,3 Wh.
- V - The supply voltage, ideally 12 V.

Determining the consumption is crucial when designing a battery array that can supply the base station with power during the hours where there is no Sun. This will be further discussed in subsection 5.3.

5.2 Positioning

The conditions in the area of operation heavily affects the performance of both solar cells and batteries. Therefore, choosing a specific position is important in order to determine the specifications. The initial requirement of operation north of the Arctic circle implicates that the autonomous base station would be designed to work with minimal insolation and in cold climates, which further implies that operating in other areas of the Nordics would be possible. Preferably the position would have plenty of meteorological data available, which would increase the accuracy in the resulting calculations.

The position chosen is the Tarfala area, located above the Arctic circle in the mountainous area south east of the Abisko National park, see figure 5.2. Located in the most northern part of Sweden, the Tarfala area experiences big differences between highest and lowest temperature, as well as the amount of insolation during the year.



Figure 5.2: Map showing the Nordic Countries and the position of the Tarfala area. Picture from Wikimedia Commons, altered with permission. Available at : <https://commons.wikimedia.org/wiki/File:Nordic-countries.png>

The Tarfala area was chosen simply because it is a remote and extreme environment north of the Arctic circle. Multiple meteorological measurements have also been conducted there over a long period of time, therefore there is plenty of data to be studied.

This project uses meteorological data from two meteorological stations located in the Tarfala area, which are both operated by SMHI (Swedish Meteorological and Hydro-logical Institute). Meteorological data supplied by the POWER (Prediction of Worldwide Energy Resource Project) project, a NASA (National Aeronautics and Space Administration) sponsored project, was also used.

The SMHI meteorological station *Tarfala A* has been measuring a number of parameters hourly since the year 1995 while the SMHI station *Tarfala Sol* was set up to monitor insolation and radiation from the Sun in 2008. The two stations are very close to each other and the measurements from both stations can therefore be combined, see Table 5.3 for exact position of both the stations. The data is public and free to use for anyone.

Table 5.3: Positioning of the two meteorological measurement stations operated by SMHI and the University of Stockholm in Tarfala [32].

| Station | Latitude | Longitude | Meters above sea level |
|--------------|----------|-----------|------------------------|
| Tarfala A: | 67.9113 | 18.6068 | 1150m |
| Tarfala Sol: | 67.9123 | 18.6101 | 1144m |

The POWER project collects meteorological data from over 200 satellites orbiting the Earth. The data is then validated and published on their GIS web application for public and commercial use. The POWER project supplies data for particular locations all over the globe and they can deliver data that stretches from each month up to 22 years of collected data.

All of the following tables regarding meteorology and solar energy are based on the coordinates of the meteorological station Tarfala A.

Table 5.4: Monthly average air temperature, lowest and highest daily average air temperature for specific month in Tarfala. Based on the measurements done by the SMHI meteorological weather station *Tarfala A* in 2016 [32].

| Month | Average monthly [C] | Lowest daily average [C] | Highest daily average [C] |
|------------|---------------------|--------------------------|---------------------------|
| January: | -12.367 | -26.4 | -4.2 |
| February: | -9.548 | -13.6 | -4.9 |
| March: | -7.471 | -14.6 | 1.2 |
| April: | -5.973 | -11.7 | 0.8 |
| May: | 0.436 | -4.4 | 8.1 |
| June: | 3.493 | -1.6 | 9.6 |
| July: | 9.048 | 3.2 | 14.1 |
| August: | 5.868 | 1.0 | 9.2 |
| September: | 3.29 | 0.2 | 9.9 |
| October: | -0.76 | -7.0 | 5.4 |
| November: | -8.05 | -14.7 | -0.6 |
| December: | -5.393 | -14.6 | 3.9 |

Table 5.5: Lowest and highest air temperature for each month in the Tarfala area. Based on the measurements done by the SMHI meteorological weather station *Tarfala A* in 2016 [32].

| Month | Lowest daily [C] | Highest daily [C] |
|------------|------------------|-------------------|
| January: | -29.3 | 0.2 |
| February: | -18.2 | -1.8 |
| March: | -17.6 | 6.1 |
| April: | -14.9 | 6.2 |
| May: | -6.9 | 10.7 |
| June: | -5.2 | 13.8 |
| July: | 2.2 | 18.3 |
| August: | -0.8 | 14.3 |
| September: | -2.3 | 12.3 |
| October: | -9.3 | 9.1 |
| November: | -17.6 | 9.1 |
| December: | -17.2 | 8.0 |

When positioning a solar powered system north of the Arctic circle, the main issue to solve is to convert as much as possible of the little insolation received in November to last during the dark period of December. As can be seen in Figure 5.3 the insolation incident on a horizontal surface is non-existent during the month of December and the same almost applies to the months of November and January. To optimize the positioning of a solar module, angles of the insolation have to be studied, in particular the *azimuth angle* (the Sun's horizontal angle when above the horizon, measured from the north (0°) counterclockwise) and the *solar elevation angle* (the Sun's vertical position in relation to the horizon, horizon equals 0°).

Firstly, the amount of energy received, in form of direct- and diffuse insolation is illustrated in Figures 5.4 and 5.5. As explained in Section 4.3.1 and Equation 4.2 the addition between these types of insolation amounts to the total insolation.

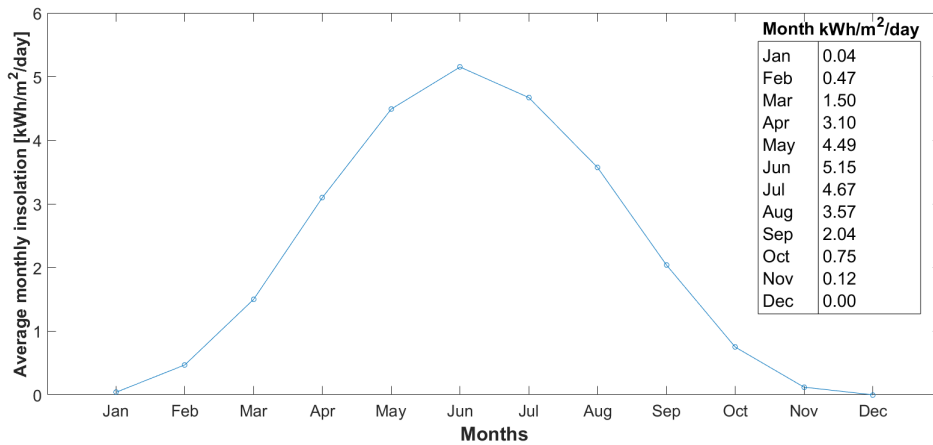


Figure 5.3: 22-year average of insolation measured on a horizontal area located in the Tarfala area. Data retrieved using the POWER database [33], using the "*Insolation on horizontal surface*".

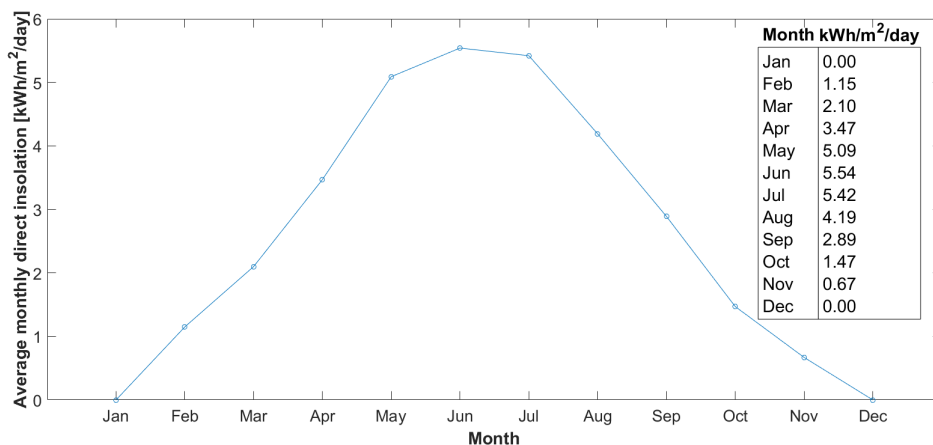


Figure 5.4: 22-year average of direct insolation, in the Tarfala area. Data retrieved using the POWER database [33], using the "*Direct normal radiation*".

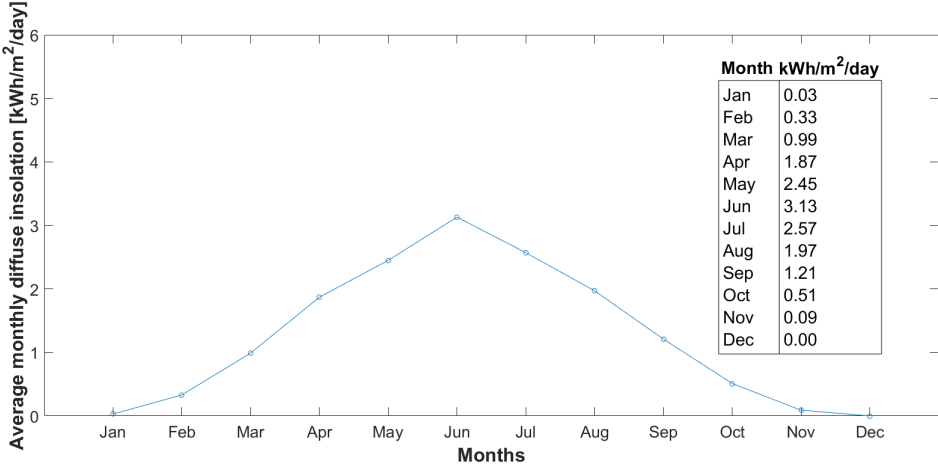


Figure 5.5: 22-year average of diffuse insolation, in the Tarfala area. Data retrieved from the POWER database [33], using the "Diffuse radiation on a horizontal surface".

Table 5.6 displays the total solar irradiance. This data is used in Chapter 6 to calculate the power output from a solar module.

Table 5.6: Solar irradiance for the chosen position in the Tarfala area. Calculated using Equation 4.2 with data from Figures 5.4 and 5.5.

| Month | $G_{TOT}[W/h]$ |
|------------|----------------|
| January: | 1.25 |
| February: | 61.67 |
| March: | 128.75 |
| April: | 222.50 |
| May: | 314.58 |
| June: | 361.25 |
| July: | 332.92 |
| August: | 256.67 |
| September: | 170.83 |
| October: | 82.50 |
| November: | 31.67 |
| December: | n/a |

Secondly, the horizontal- and vertical angles of the Sun as well as the relation between them are illustrated in Figures 5.6, 5.7 and Table 5.8. Figure 5.6 displays the *cardinal directions* of the Sun’s journey above the horizon in the region, as referenced from the true north. Measured as an average for every hour of the month, the graphical representation in Figure 5.6 is instrumental when choosing the cardinal direction of the solar module.

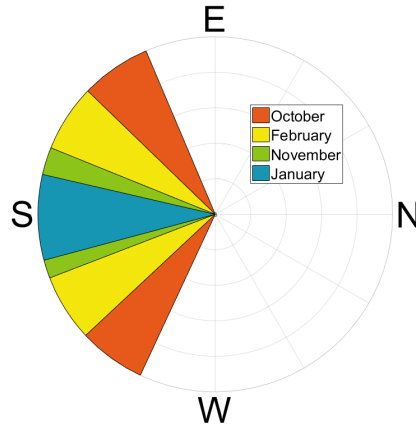


Figure 5.6: Coloured area represents the cardinal directions of the Sun's position above the horizon during the months of October, November, January and February in the Tarfala area. The months are subsets to each other in the following order; October, February, November, January. Data retrieved from the POWER database [33], using the "*Hourly solar azimuth angles*". Data adjusted for UTC+1.

Table 5.7: Azimuth angle at sunset for October, November, January and February. Data retrieved from the POWER database [33], using the "*Hourly solar azimuth angles*". Data adjusted for UTC+1.

| Month | Azimuth angle at sunset |
|-----------|-------------------------|
| October: | 245° |
| November: | 201° |
| January: | 195° |
| February: | 223° |

Table 5.8 provides information on the Earth's rotation from the point where the Sun reaches its highest elevation on the local *meridian* to the *sunset*. This information is necessary when determining the azimuth angle of the Sun's position that correlates to the peak solar elevation angle.

Table 5.8: Monthly average number of degrees the Earth has rotated from *solar noon* to *sunset* θ_s . Data retrieved from the POWER database [33], using the "*Sunset hour angle*". Data adjusted for UTC+1

| Month | Average rotation in degrees |
|-----------|-----------------------------|
| October: | 68.5° |
| November: | 35.9° |
| January: | 20.8° |
| February: | 57.2° |

Figure 5.7 displays the height the Sun reaches during the darker months of October, November, December, January and February, with June (brightest month) as a reference. This data is important when determining the vertical angle of the solar module.

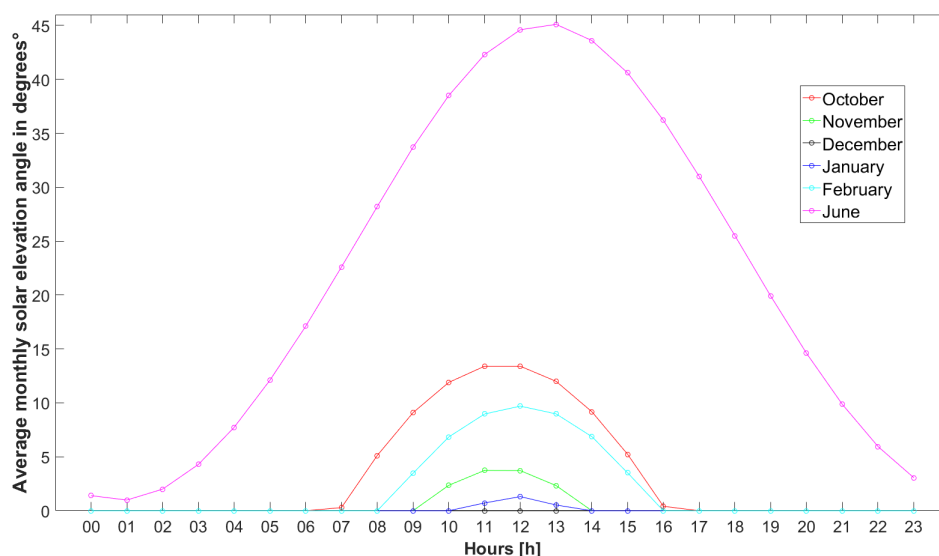


Figure 5.7: Solar elevation angle in the Tarfala area for the October, November, December, January, February and June. Data retrieved from the POWER database [33], using the "Hourly solar angles relative to the horizon". Data adjusted for UTC+1

Lastly, according to the POWER database [34] for measurement of the "Insolation on Horizontal Surface" on a daily average, there is no insolation at all from **December the first** to **January the tenth**. This amounts to 41 days of complete darkness.

5.2.1 Angle of solar module

In Section 5.2 a few important angles were discussed that play a big role in the optimal positioning of the module. Allowing the solar radiation to hit the solar module at a 90° angle, called direct insolation, is desired due to the concept discussed in Section 4.3.1 and Figure 4.6. This concept is further strengthened by Figure 5.4 showing the direct insolation for the same location as in Figure 5.3 which is clearly stronger during all months except January, when the Sun barely reaches above the horizon. Thus to maximize the generated energy, the solar module should be directed in a *solar elevation- and azimuth* angle favouring direct insolation while also maximizing the time exposed to solar radiation. Ideally these two conditions would correlate, however there is a slight difference that will be described below. By just looking at Figure 5.6 it could be assumed that 180° , or *south*, would be an optimal direction to maximize the exposed time. To calculate the average azimuth angle for each month, as seen in Table 5.9, the raw data which Figure 5.6 is based on is used.

Table 5.9: Azimuth angle average α for October, November, January and February.

| Month | Azimuth angle average |
|-----------|-----------------------|
| October: | 179° |
| November: | 180° |
| January: | 181° |
| February: | 180° |

The angles in Table 5.9 average to 180° which equals a south direction, in other words positioning the solar module directly south would maximise the time exposed to solar radiation.

To maximise the direct insolation, an azimuth angle correlating to the peak solar elevation angle must be calculated. This azimuth angle is not necessarily the same as the angle maximising the exposed time.

By using the raw data from Figure 5.6 and subtracting the angles θ_s in Table 5.8 from the *azimuth angle of the sunset* α_{sunset} for the corresponding months as seen in Equation 5.2

$$\alpha_{peak} = \alpha_{sunset} - \theta_s \quad (5.2)$$

Table 5.10 shows the results of this calculation describing the Sun's horizontal position when it reaches its highest elevation above the horizon.

Table 5.10: Peak azimuth angle average α_{peak} for October, November, January and February.

| Month | Azimuth angle for peak solar elevation angle |
|-----------|--|
| October: | 176.5° |
| November: | 165.1° |
| January: | 174.2° |
| February: | 165.8° |

The angles in Table 5.10 average to 170.4° which equals a *south by east* direction slightly differing from the direction maximizing the exposed time.

Achieving optimal positioning of the solar module is simplified by the delimitation of only studying the insolation during the the darker months of October to February, the reasoning for this as seen in Section 5.2. Hence, the resulting horizontal position narrows down to a range of 170.4° to 180° angles, as seen when measured clockwise from the north (0° angle). Regardless of where the solar module is positioned in the concluded horizontal range, maximizing the insolation normal to the module, a 90° vertical position will be needed. Studying Figure 5.7, the curves represents the height the Sun reaches above the horizon at which time. Optimising for the darkest period of year requires a very steep vertical angle to "catch" the insolation, hence the 90° vertical angle when measured from the horizon and up.

To conclude, positioning the solar module 170.4° *south by east* horizontally and 90° vertically would maximise the direct insolation.

5.3 Choosing the right equipment

Choosing the right equipment is a trade-off between performance, cost and sustainability. Due to the nature of this project, performance and cost are prioritised because a higher maintenance solution would render the project purposeless. Also, choosing components with less environmental impact would have little effect because of the size of the system. To sum up, the project focuses on high performance with small means.

In this section the reasoning behind what equipment has to be used and why will be presented, divided into two subsections, one concerning the solar modules and one concerning the type of battery needed.

5.3.1 Solar Module

In Section 4.3.1 it was concluded that the insolation in the Nordic countries is limited during the period between the autumn equinox and the spring equinox due to the axial tilt of the Earth. This implies that at a given position in the Nordic countries, a solar module with a specific size will receive less energy per area unit than a solar module positioned with more

direct sunlight (solar radiation normal to the surface of the Earth). Considering the low energy solar radiation for much of the year and the band gap energy levels explained in Section 4.3.2.1, a lower band gap energy level is preferred as it would allow the solar module to absorb more of the low energy radiation.

While lower band gap energy would allow for more low-energy radiation to be converted, it also converts less of the high-energy radiation. The *Shockley-Queisser limit* illustrated in Figure 5.8 relates the efficiency to the band gap energy level [36]. It can be seen that an optimal band gap energy level would correspond to $\sim 1.34\text{eV}$, with monocrystalline silicon having a slightly lower energy level at $\sim 1.1\text{eV}$, as explained in Section 4.3.2.1.

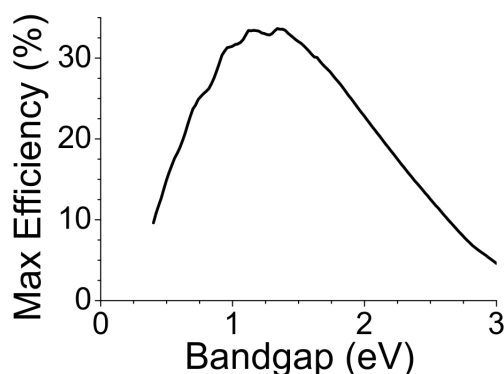


Figure 5.8: Conversion efficiency in relation to band gap energy level. Picture from Wikipedia commons, public domain. Available: <https://commons.wikimedia.org/wiki/File:ShockleyQueisserFullCurve.svg>

However, adding the above reasoning regarding low-energy radiation with the availability and reliability of monocrystalline silicon solar cells, it narrows down to the best choice for this application. Assuming a specification based on a product on the market will help in achieving simulated power levels, attainable in the chosen environment. The *bSolar* solar cell is an efficient monocrystalline silicon cell, producing a good amount of current. A few chosen specifications are shown in Table 5.11, the complete data sheet is found in [35].

Table 5.11: Chosen specifications from data sheet of the monocrystalline silicon solar cell *bSolar TG18.5 BR BIN 36*.

| Electrical data (STC) | Value |
|----------------------------------|--------------|
| Open-circuit voltage V_{OC} : | 0.62V |
| Short-circuit current I_{SC} : | 8.88A |
| Max power P_{MAX} : | 4.39W |
| Temp. coefficient voltage : | -0.00223V/°C |

Determining the specifications for a solar module that operates for the entirety of the year increases in difficulty the further it is positioned from the equator, due to the variation in solar radiation. Considering the specifications of the single solar cell found in Table 5.11, the cell produces ample amounts of current and a significantly smaller voltage. Solar modules typically consists of several cells connected in series (36 is common off-the-shelf) to increase the voltage and few connected in parallel (if any) to increase the current. However, due to the short-circuit current's I_{SCG} linear dependence of of the solar irradiance (section 4.3.2.2), the generated current in June is more then ten times the generated current in November. Considering the chosen location, designing a solar module providing $\sim 6\text{A}$ in November would generate $\sim 70\text{A}$ in June, thus causing problems related to heating of the components. The issue of these high currents can be solved using a proper charger/regulator as discussed in Section 4.2.2.4.

Applying the methodology described in Section 4.3.2.2 to attain a relation between the current and voltage, while accounting for temperature, solar irradiance and electrical losses, a result can be obtained. In Chapter 6 the solar module capacity will be put in to relation with the battery capacity and consumption of the Sigfox base station.

5.3.2 Battery

To power the base station when the solar module is unable to produce power due to the lack of solar irradiance, the system requires a battery as a backup power supply.

This section will explain which technologies and battery types that will be suitable as backup power for the system. It will also include the tools necessary to determine the size of the battery. These "tools" can be used for choosing the right battery size for backup energy anywhere in the Nordic countries.

5.3.2.1 Type of battery

Since the Sigfox SBS-T3-868 is designed to work with a 12 VDC supply the power backup system will be designed using a 12 V battery.

To ensure that the battery can charge during the times with colder climate (below 0 °C) a battery of the lead-acid type is the only option since the Tarfala area can experience very low temperatures during winter time, see Table 5.5. As explained in Section 4.2.2.3 a battery of the lead-acid type can still be operational when the temperature of the electrolyte is -20 °C. With the addition of the insulation of the battery package and the heat that builds up inside the battery when used this will be enough to guarantee that the battery can operate even during the coldest periods. This is of course also the case in many other areas in the Nordic countries, as many areas both in the southern and the northern parts can experience very low temperatures during winter time.

To be able to design a system that is as maintenance free as possible the battery has to have an extended lifetime expectancy and preferably be of the type that can handle deep levels of discharge during the darkest times without taking excessive damage. The best solution for this is to use a battery of the *deep cycle* type. As explained in Subsection 4.2.2.5 a lead-acid battery of the deep-cycle type allows the energy to be drained all the way down to 80% of the total capacity without causing excessive damage to the battery cells.

5.3.2.2 Battery capacity

The capacity of a battery is commonly determined by the amount of ampere hours (Ah) a battery contains while fully charged. One ampere hour means that the battery can supply one ampere during one hour of continuous operation.

To be able to calculate the capacity needed for the battery, the amount of ampere hours used to power the base station during the hours when there is no sunlight has to be decided. This is done by using Equation 5.3 and the data provided by the POWER project (see Section 5.2). By typing in the longitude and latitude of the location where the base station is to be placed into the POWER project tools one can easily obtain data showing the amount of sunlight in the specific location during the whole year. Here it is important to choose the day/days with the least amount of sunlight to ensure that the battery is configured so that it has enough capacity to power the base station during the darkest day of the winter.

$$I_{Consumption} = \frac{P_{Consumption}}{V_{Ideal}} \times T_{Hours} \quad (5.3)$$

The parameters in Equation 5.3 are the following:

- $I_{Consumption}$ - The amount of ampere hours [Ah] needed to power the base station during the darkest time.
- $P_{Consumption}$ - The rate of power consumption [W] of the base station. For the Sigfox SBS-T3-868 it is 17,3 W.
- V_{Ideal} - The supply voltage [V] ideally consumed by the base station. For the Sigfox SBS-T3-868 it is 12 V.
- T_{Hours} - The longest continuous time of darkness the location experiences during the year.

In order to determine the actual capacity needed for the battery, the *minimum charge factor* must be considered. Equation 5.4 solves this. The minimum charge factor is based on the depth of discharge allowed by the chosen battery and it is included to make sure that the battery is not discharged completely when the system is heavily reliant on the power supply of the battery. If the battery is completely discharged it could lead to permanent damage, as explained in Subsection 4.2.2.5. Even deep cycle lead-acid batteries have minimum charge factors and therefore the equation do not have a set value since it depends on the characteristics of the chosen battery.

$$I_{Size} = I_{Consumption}(1 + MinCharge) \quad (5.4)$$

The parameters in Equation 5.4 are the following:

- I_{Size} - The amount of ampere hours [Ah] required.
- MinCharge - The minimum charge recommended for the chosen battery, measured in percentage %.

6

Results

Due to the lack of solar energy above the Arctic circle during the winter months and the fact that the Sigfox SBS-T3-868 base station consumes a considerable amount of energy, the resulting conclusion is that there is no practical solution for the establishment of an autonomous solar powered Sigfox SBS-T3-868 base station north of the Arctic circle. The purpose of this section is to explain the reason for this and the difficulties faced that ultimately led to this result.

For the purpose of providing a summary of parameters to consider when designing a solar powered system for the Nordic countries, one section will be dedicated to providing the universal technologies and tools necessary for this.

6.1 Autonomous above the Arctic circle

In Chapter 2 three requirements were emphasised, these were:

- Solar powered
- Low maintenance
- Easy to assemble and disassemble

Below is a follow-up to these requirements and how they do not collaborate under the circumstances faced in this project.

A solar module consisting of 36×2 solar cells is considered large in this context, amounting to approximately $0.63m \times 2.81m$ if positioned vertically. To maintain the requirement of *Easy to assemble and disassemble*, a larger module is impossible considering the limitation in transporting and mounting the module. Therefore the calculations will be based on a 36×2 -solar module, which is a common and readily available size [37].

By considering the measured consumption in Table 5.2, and Figure 6.1 illustrating the output from a 36×2 -solar module based on the solar cell found in Table 5.11, it can be seen that the period of November throughout January can not match the consumption requirements of the base station.

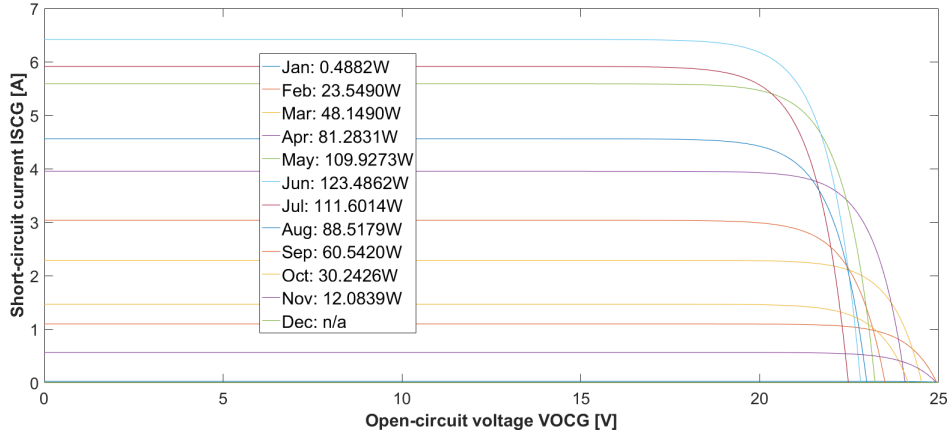


Figure 6.1: I-V plot for all the months of the year, using a 36×2 -solar module. Legend shows the *MPP* for the conditions faced during each month, June provides the best conditions with December and January supplies close to nothing in terms of power. Calculations based on Equation 4.3 and data from Tables 5.6 and 5.4

If the calculations were solely based on the consumption of the base station, the module would have to grow in parallel to produce enough current for **November** and **January**. This would quickly escalate to an unreasonable size. Hence the fact that the requirement of *Solar powered* excludes *Easy to assemble and disassemble*. Therefore the calculations resulting in Figure 6.1 serves as an example to illustrate the difficulty of powering the Sigfox SBS-T3-868 base station.

As stated in Section 5.3.2.2 the capacity of the battery backup must coincide with the consumption during the period with no- or limited sunlight. According to Figure 6.1, the period of **November** to **January** fails to satisfy the consumption of the base station, this period is therefore the longest period the battery needs to power the base station.

The three months (92 days) expressed in hours translates to *2208 hours*.

Using this time period as $T_{Hours} = 2208h$ in Equation 5.3, yields the result $I_{Consumption} = 3183.2Ah$.

Adjusting the capacity to account for the *minimum charge factor* as in Equation 5.4 results in $I_{Size} = 3819.84Ah$.

Since there are no batteries of that size, an array would have to be built. However, since both the size and costs would be too large we can conclude that there is no practical way of building a *Low maintenance*, autonomous system for the Sigfox SBS-T3-868 base station north of the Arctic circle.

6.2 Universal technical parameters

While compiling the research done to reach this result, certain methods and equipment optimised for the projects scope could be regarded as applicable in most conditions faced in the Nordic countries. These parameters can be regarded as universal technical parameters for establishing an autonomous Sigfox base station in the Nordic countries.

6.2.1 Battery technology

As explained in Subsection 4.2.2.3 and Subsection 5.3.2.1 a battery of the lead-acid type has to be used for this type of application in order to ensure that the system can stay operational

during the coldest time periods.

For highest possible efficiency the lead-acid battery should be of the deep-cycle type, since this allows for deeper depth of discharge and has a greater lifetime expectancy, making more efficient use of the total capacity of the battery and making the system as maintenance free as possible, explained in Subsection 4.2.2.5 and Subsection 5.3.2.1.

As explained in Subsection 4.2.2.2 batteries also have a self-discharge factor, it would therefore be preferable that the chosen lead-acid battery of the deep-cycle type that has the smallest possible self-discharge rate to ensure a minimal energy loss.

6.2.2 Solar module

Using a monocrystalline silicon solar cell has the benefits of being a well proven technology with high reliability. For the specific environment there are efficiency-related advantages with this technology as significantly improved performance in cold weather as well as high conversion of low-energy radiation. Explained in Sections 4.3.2.1 and 4.3.2.2.

Positioning the solar module to maximise the direct insolation is vital. Although the exact optimal position needs to be studied for each position, some general assumptions can be made. A 90°(or near) vertical angle is required to absorb as much of the radiation during winter when the solar elevation angle is lower towards the horizon. Horizontally the solar module must be positioned to the *south* or *south by east* to allow the Sun's rays to hit the module at its peak solar elevation angle, which correlates to peak insolation. Explained in Section 5.2.1.

6.2.3 Power regulator

A power regulator is needed to ensure that the charging current transmitted to the battery is adapted to the battery's current state. If the same current were to be transmitted to the battery from the solar module all the time, the battery would be damaged or not charged properly, as explained in Section 4.2.2.4. Many power regulators made for PV-applications also function as a power relay [38].

The power relay function in the regulator measures the amount of energy produced by the solar module and determines if the solar module can drive the load directly or if the focus should be on charging the battery. If the battery is fully charged the power will be redirected to drive the load directly. This function prolongs the battery lifetime, as explained in Section 4.2.2.4.

7

Discussion

Considering the inherent low-power characteristic of the LPWAN and its ability to provide coverage for large areas, the possibility of an autonomous above-the-arctic-circle application seems feasible. This section will attempt to pinpoint the areas of improvements and also discuss other similar projects with possibly adaptable solutions to the issues faced in this project. Initially though, some assumptions related to limited accuracy of insolation data were made, these will be presented as well.

7.1 Methods

The used data concerning insolation provided by the POWER project only shows the monthly average, which does not give sufficiently detailed information about the amount of energy that can be harvested during the darkest periods. Hence the calculations used to determine the possible solar power output and battery capacity have a reasonable amount of uncertainty. The albedo effect have not been taken into account, since we found no data concerning the impact of this effect for the Tarfala area. Since the albedo effect is something that would have a different impact on the system design depending on the region, it is difficult to design a system relying on it. For a specific area, in particular the northern areas of the Nordic countries, the impact of the albedo effect would have to be further studied by conducting field tests. A series of measurements in the chosen area would have to be done in order to achieve the best system optimisation.

When analysing the temperature of the Tarfala area the data of the year 2016 was used. In comparison to the POWER database SMHI do not provide data that shows an average over longer time periods. The data provided shows the temperature for hours, days and monthly average, so more time could have been spent on summarising the average temperature data for a longer time period, like the 22-year period in the POWER database. This could give a more accurate representation of the area. However, this do not change the fact that the area experiences periods of extreme cold, which means that the battery would still have to be of the lead-acid technology.

It is necessary to assume that the data regarding direct- and diffuse insolation correlates to the positioning of the module, which was explained in Section 5.2.1. However, this is not entirely true. The reason for this is that the module is optimised for the period of **October** to **February**. This implies that the power output for the period **March** to **September** is exaggerated as the module is not optimised for direct insolation during that period. Nonetheless, this is a small issue and does not affect the result as the conditions during the period **March** to **September** are non-problematic.

During the project we have also analysed the possibilities of positioning the system in the southern parts of Sweden. When we examined the possibility of a system designed for placement in *Smygehuk* the requirements were still unrealistic in terms of size and cost of the battery.

7.2 Improvements

The main area of improvement can be traced to the power consumption of the Sigfox SBS-T3-868 base station. In order to reduce the consumption, the base station would have to be redesigned.

However, Sigfox already supplies an option to the SBS-T3-868 base station. The Sigfox licensed operator in Australia, a company called *thinstra*, provides a complete solar powered system based on a different base station, the *Sigfox Mini*. The Sigfox Mini can handle less amount of data traffic, but it is also more energy efficient and smaller in size [39]. Unfortunately the conditions for Australia do not apply in the Nordic countries, and the already operational *thinstra* system can not be adopted to match the conditions of the Nordic countries without redesigning the system. This base station could be an interesting component to study in order to determine whether it could be used to design an autonomous system for the Nordic countries.

A few years ago, a project aimed to monitor the movement of reindeer herds using a LoRa network was conducted. The project was led by Peter Selemark, owner of Sanibel Management. Selemark developed a LoRaWAN base station completely reliant on a 25W solar module with a 55Ah battery backup for the dark period of the year. These stations were spread out over northern Sweden, with the northernmost station positioned at 68.35127, 19.88739, therefore experiencing complete darkness for over a month each year. A few translated outtakes from the conversations we have had with Peter Selemark is found below, as well as our thoughts on how his ideas and field experience could improve the solution for powering a Sigfox base station.

'It [The base station] was extremely optimised for low power consumption'

Low power consumption was the main goal and dominated the choices of components.

'It [The base station] was operational for 52- out of every 60 minutes.'

By limiting the up-time, a significant decrease in power consumption was achieved.

'The initial application was monitoring of reindeer. For the majority of the year they are located in areas without cellphone coverage or electrical grid connectivity. Together with the reindeer herding Sami people, we operated deep inside the national parks. Our base stations (I have built approximately 55 stations) operated completely from solar power and a battery.'

The base station's purpose was to monitor reindeer and possibly other animals, hence the optimisation for this specific application. This might imply limitations during other circumstances, which makes a comparison with the Sigfox SBS-T3-868 base station difficult. However, taking notice from Peter Selemark's research, it is easy to argue that the problem resulting in our negative outcome is best solved by lowering the base station's power consumption. This may lead to a decreased functionality, although with the specific requirement of operation north of the Arctic circle, a compromise on functionality seems reasonable.

Another aspect that could be further studied is the use of wind turbines as a compliment to the solar modules. If a wind turbine could provide energy during the darkest periods and help charge the battery, the total size and capacity of the battery could probably be decreased. This would help to move the project closer to operation north the Arctic circle. However, since a

wind turbine has a lot of moving parts which tend to imply increased maintenance, this trade-off have to be further studied. As with solar power, a wind turbine is highly dependant on location, we recommend using the SMHI (or equivalent) databases to analyse the conditions for the specific area in order to determine its potential.

7.3 Final thoughts

Even though the result was negative we still believe that the future implementation of a LPWAN network in rural areas of the Nordic countries should be something to strive for. The amount of areas that could benefit from data gathering in hard-to-reach places are many. Supplying coverage in these areas could greatly benefit both economical- and environmental interests since unsupervised changes in the environment, the flora and fauna, etc. could easily become autonomously monitored.

One actual case is the currently ongoing bachelor thesis by Mattias Blinge, "Monitoring movement of the Atlantic Salmon wirelessly using Sigfox LPWAN" (working title) at Chalmers University of Technology. In the project Blinge uses a Sigfox modem to provide wireless communication to a tracking sensor used in the international "Smolt tracking project". During the project Blinge experienced package loss due to poor coverage in the area where the Sigfox modem was placed. An autonomous base station providing coverage off-the-grid would solve these kind of problems and make it possible to monitor cases like Blinge's.

Bibliography

- [1] Walters Nyambi, "The IoT Revolution: challenges and opportunities", Geneva Business News, 11-07-2016, [Online], Available:
<https://www.gbnews.ch/the-iot-revolution/>, [Accessed: 31/05-2018].
- [2] S. Al- Sarawi, M. Anbar, K. Alieyan and M. Alzubaidi, "Internet of Things (IoT) communication protocols: Review", in Proceedings of the 8th International Conference on Information Technology (ICIT), 17-18 May, 2017, Amman, Jordan. IEEE Explore, IEEE, 2017. Available:
<https://ieeexplore-ieee-org.proxy.lib.chalmers.se/document/8079928/>, [Accessed: 3/5 - 2018].
- [3] D. Cliff, "Cellular, LPWAN Challenge Short-Range Wireless Solutions in IoT Markets", Microwave Journal, International ed.; Dedham, Volume 60, Issue 7, Jul 2017. Available:
<https://search.proquest.com/docview/1919916392/fulltext/99F0BA3385A14599PQ/1?accountid=10041>, [Accessed: 01/05-2018]
- [4] M. Rouse, S. Shea and M. Haughn, "LPWAN (low power wide area network)", TechTarget - IoT Agenda, 09 - 2017, [Online], Available:
<https://internetofthingsagenda.techtarget.com/definition/LPWAN-low-power-wide-area-network>, [Accessed: 25/04-2018].
- [5] Wikipedia contributors, "ISM band", [Online], Available:
https://en.wikipedia.org/wiki/ISM_band, [Accessed: 03/04-2018].
- [6] Official Journal of the European Union,"Commission implementing decision (EU) 2017/1483" ,[Online],Available:
<http://eur-lex.europa.eu/legal-content/EN/TXT/?qid=1519682383896&uri=CELEX:32017D1483>, [Accessed: 26/04-2018].
- [7] J-P. Bardyn, T. Melly, O. Seller and N. Sornin, "IoT: The era of LPWAN is starting now", European Solid-State Circuits Conference, ESSCIRC Conference 2016: 42nd, 12-15 Sept. 2016. [Online], Available:
<https://ieeexplore.ieee.org/document/7598235/>, [Accessed: 01/05-2018]
- [8] K. Mekkia, E.Bajica, F. Chaxela and F. Meyer,"A comparative study of LPWAN technologies for large-scale IoT deployment", ICT Express, 21 Sep-2017. [Online], Available:
https://www.sciencedirect.com/science/article/pii/S2405959517302953?_rdoc=1&_fmt=high&_origin=gateway&_docanchor=&md5=b8429449ccfc9c30159a5f9aeaa92ffb, [Accessed: 10/05-2018]
- [9] Wikipedia contributors, "Short-range device", [Online], Available:
https://en.wikipedia.org/wiki/Short-range_device#SRD860, [Accessed: 04/04-2018].

- [10] Sigfox, 'Our Vision', [Online]. Available: <https://www.sigfox.com/en/our-vision>, [Accessed: 27/03- 2018].
- [11] G. Schatz, 'SigFox Vs. LoRa: A Comparison Between Technologies & Business Models', 13/01-2016. [Online]. Available: <https://www.link-labs.com/blog/sigfox-vs-lora>, [Accessed: 27/03-2018].
- [12] Sigfox, "Radio configuration", [Online], Available: <https://resources.sigfox.com/document/radio-configuration>, [Accessed: 04/04-2018].
- [13] IoT Sweden, "Sigfox - Nätverket", [Online], Available: <https://www.iotsweden.net/sv/natverket/>, [Accessed: 26/04-2018]
- [14] Sigfox, "Technical Overview", [Online], Available: <https://www.disk91.com/wp-content/uploads/2017/05/4967675830228422064.pdf>, [Accessed: 4/4-2018]
- [15] Sigfox, "Radio technology - Ultra Narrow Band", [Online], Available: <https://www.sigfox.com/en/sigfox-iot-radio-technology>, [Accessed: 4/4-2018]
- [16] C. Julien, A. Mauger, A. Vijn and K. Zaghbi, *Lithium Batteries - Science and Technology*, 2016, Springer. [Online], Available: <https://link.springer.com/book/10.1007%2F978-3-319-19108-9>, [Accessed 23/02-2018].
- [17] P. Detchko, "Lead-Acid Batteries - Science and Technology - A Handbook of Lead-Acid Battery Technology and its Influence on the Product (2nd Edition)", 2017, Elsevier, Amsterdam, Netherlands. [Online], Available: https://app.knovel.com/web/toc.v/cid:kpLABSTA06/viewerType:toc/root_slug:lead-acid-batteries---science-and-technology---a-handbook-of-lead-acid-battery-technology-and-its-influence-on-the-product-2nd-edition/url_slug:front-matter?&issue_id=, [Accessed: 06/05-2018]
- [18] C. Liu, Z. G. Neale and G. Cao, "Understanding electrochemical potentials of cathode materials in rechargeable batteries", *Materials today* vol.19 issue 2, pp. 109-123, March 2016, [Online], Available: <https://www.sciencedirect.com/science/article/pii/S1369702115003181>, [Accessed: 25/02-2018].
- [19] J. Jung, L. Zhang and J. Zhang, "Lead-acid Battery technologies, Fundamentals, Materials, and Applications", 2016, CRC Press, Taylor & Francis group, 6000 Broken Sound Parkway, New York, Suite 300. [Online], Available: <https://www-taylorfrancis-com.proxy.lib.chalmers.se/books/9781466592230>. [Accessed: 06/05-2018].
- [20] I. Buchmann, "BU-410: Charging at High and Low Temperatures", September, 2017. [Online], Available: http://batteryuniversity.com/learn/article/charging_at_high_and_low_temperatures. [Accessed: 07/05-2018].
- [21] All About Lead Acid Batteries, "Three Stage Battery Charging". [Online], Available: <http://all-about-lead-acid-batteries.capnfatz.com/all-about-lead-acid-batteries/lead-acid-battery-charging/three-stage-battery-charging/>, [Accessed: 1/6-2018]

- [22] Dr. D. H. Hathaway, "The Solar Interior", 2015, NASA. [Online], Available: <https://solarscience.msfc.nasa.gov/interior.shtml> [Accessed: 25/03-2018]
- [23] R. Rösemann, "A Guide to Solar Radiation Measurement: From Sensor to Application", 2nd ed.: Kipp Zonen, 2011. [Accessed: 25/03-2018]
- [24] P. R. Gringer, "EM spectrumrevised", licensed under the Creative Commons Attribution-Share Alike 3.0 Unported. [Online], Available: https://commons.wikimedia.org/wiki/File:EM_spectrumrevised.png, [Accessed: 21/04-2018]
- [25] H. Karttunen, P. Kröger, H. Oja, M. Poutanen, K.J. Donner, "The Solar System" in *Fundamental Astronomy*, New York: Springer-Verlag, 1987. [Online], Available: https://link.springer.com/content/pdf/10.1007%2F978-1-4612-3160-8_2.pdf [Accessed: 18/04-2018]
- [26] P. Halasz, "Oblique rays", licensed under the Creative Commons Attribution-Share Alike 3.0 Unported. [Online], Available: http://commons.wikimedia.org/wiki/File:Oblique_rays.svg [Accessed: 26/03-2018]
- [27] G. De Martino, "Effect of Germanium in Silicon for Solar Applications" Chapter 2, Norwegian University of Science and Technology, 2016. [Online], Available: <https://brage.bibsys.no/xmlui/handle/11250/2405155> [Accessed: 12/06-2018]
- [28] Vicphysics Teachers' Network Inc., 2005, With permission from Dan O'Keeffe at the Vicphysics Teachers' Network. [Online], Available: <http://www.vicphysics.org/documents/events/stav2005/spectrum.JPG>, [Accessed: 22/03-2018]
- [29] E. Lorenzo, "Solar Electricity: Engineering Of Photovoltaic Systems", 1994, PROGENSA. [Online], Available: https://books.google.se/books?id=1Yc53xZyxZQC&pg=PA78&redir_esc=y#v=onepage&q&f=false. [Accessed: 02/05-2018]
- [30] K. Mertens, G. Roth, "Photovoltaics: Fundamentals, Technology and Practice", 2014, John Wiley Sons. [Online], Available: <http://library.books24x7.com.proxy.lib.chalmers.se/assetviewer.aspx?bookid=63677&chunkid=780545582&rowid=150>. [Accessed: 24/04-2018]
- [31] Sigfox, "Sigfox SBS-T3 Product Manual", [Online], Available: <https://fccid.io/2ACK7SBST3902/User-Manual/User-Manual-3273284>, [Accessed: 29/03-2018]
- [32] SMHI Meteorological Measuring stations, Available: <https://opendata-download-metobs.smhi.se/explore/?parameter=0>, [Accessed: 04/01-2018].
- [33] POWER webpage, Available: <https://eosweb.larc.nasa.gov/cgi-bin/sse/grid.cgi?email=skip@larc.nasa.gov>, [Accessed: 04/01-2018].
- [34] POWER webpage, Available: <https://eosweb.larc.nasa.gov/cgi-bin/sse/daily.cgi?email=skip@larc.nasa.gov> [Accessed: 04/24-2018]

- [35] bsolar GmbH, "Monocrystalline Silicon Solar Cell" [Online] Available:
http://www.b-solar.com/Pictures/Monofacial%20TG18.5BR_D200.pdf
, [Accessed: 02/05-2018]
- [36] S. Rühle, "Tabulated values of the Shockley–Queisser limit for single junction solar cells", Science Direct, 2016, Elsevier Ltd. [Online], Available:
<https://www.sciencedirect.com/science/article/pii/S0038092X16001110>
, [Accessed: 18/04-2018]
- [37] S. Matasci, "What is the average solar panel size and weight?", Energysage, 2018. [Online], Available:
<https://news.energysage.com/average-solar-panel-size-weight/>
, [Accessed: 20/5-2018]
- [38] Morningstar Corp., "White papers and Documents", 2018. [Online], Available:
<https://www.morningstarcorp.com/white-papers/>
, [Accessed: 12/05-2018]
- [39] Sigfox, "Sigfox Mini base station Installation guide", [Online], Available:
<https://fccid.io/2ACK7SMBST/User-Manual/USERS-MANUAL-2988577>
, [Accessed: 06/05-2018]